*Revised Manuscript with track changes

Nuclear Met promotes hepatocellular carcinoma tumorigenesis and metastasis by upregulation of TAK1 and activation of NF-κB pathway

Sze Keong Tey[1], Edith Yuk Ting Tse[1], Xiaowen Mao[1], Frankie Chi Fat Ko[1], Alice Sze Tsai Wong[3], Regina Cheuk-Lam Lo[1,2], Irene Oi-Lin Ng[1,2], Judy Wai Ping Yam[1,2*]

[1]Department of Pathology, Li Ka Shing Faculty of Medicine, The University of Hong Kong, Hong Kong; [2]State Key Laboratory for Liver Research, The University of Hong Kong, Hong Kong; [3]School of Biological Sciences, The University of Hong Kong, Hong Kong

Corresponding author

Judy Wai Ping Yam

Department of Pathology, The University of Hong Kong, University Pathology Building, Queen Mary Hospital, Hong Kong.

Tel: (852) 2255-4864; Fax: (852) 2218-5212; E-mail: judyyam@pathology.hku.hk

Abstract

Presence of Met receptor tyrosine kinase in the nucleus of cells has been reported. However, the functions of ~~nuclear~~ Met which expresses in the nucleus (nMet) remain elusive. In this study, we found that nMet was increased in 89% of HCC tumorous tissues when compared with the corresponding non-tumorous liver tissues. nMet expression increased progressively along HCC development and significantly correlated with cirrhosis, poorer cellular differentiation, venous invasion, late stage HCC and poorer overall survival. Western blot analysis revealed that nMet is a 48-kDa protein comprising the carboxyl terminal of Met receptor. Induced expression of nMet promoted HCC cell growth, migration and invasiveness *in vitro* and tumorigenesis and pulmonary metastasis *in vivo*. Luciferase assay showed that nMet activated NF-κB pathway. Indeed, p-IKKα/β and nuclear p-p65 were higher in nMet stable cells than in the control cells. Perturbation of TAK1/NF-κB axis abrogated the aggressiveness of HCC cells, both *in vitro* and *in vivo*. In conclusion, nMet was overexpressed and as a potential prognostic biomarker of HCC. Functionally, nMet accelerated HCC tumorigenesis and metastasis via the activation of TAK1/NF-κB pathway.

Highlights

- nMet is overexpressed in human HCCs and is a potential prognostic factor for HCC patients
- nMet is a truncated cytoplasmic domain of Met surface receptor
- nMet promotes HCC tumorigenesis and metastasis *in vivo*
- Crosstalk between nMet and TAK1/NF-κB pathway leading to the aggressiveness of HCC cells

Keywords

Hepatocellular carcinoma, Metastasis, Nuclear factor kappa B, Nuclear Met, Transforming growth factor beta-activated kinase 1

1. Introduction

Met receptor tyrosine kinase (RTK) is a cell surface single-pass heterodimer comprising a glycosylated extracellular α subunit linked by a disulfide bond to a transmembrane β subunit. Upon binding with its native ligand hepatocyte growth factor (HGF), Met dimerizes and autophosphorylates the cytoplasmic kinase domain, which eventually activates the bidentate substrate binding site and triggers various downstream signaling cascades [1]. Under normal conditions, the HGF-Met axis contributes indispensably with other cytokines and growth factors to coordinate optimal nerve development, liver regeneration, morphogenesis, embryonic development and wound healing [2-5]. However, signaling pathways kindled by aberrant HGF-Met axis orchestrate to switch on the invasive growth program, thereby promoting tumorigenesis, angiogenesis and metastasis in many cancers. Expression level of Met is consistently associated with the progression of different cancers and upregulation of Met is frequently observed in metastatic tumors [6].

Various RTKs, such as ErbB1 and ErbB4, have been reported to translocate into nucleus of cells as either intact or truncated forms [7, 8]. These receptors exert multifaceted functions in different subcellular localizations [9]. Nuclear Met (nMet) was first reported in melanoma tumors and cell lines [10] and was later found in different malignancies, including breast, lung, oral and prostate carcinoma [11-18]. In breast carcinoma, nMet is predictive of poor outcome [12, 19]. These observations suggest the involvement of nMet in oncogenesis. It is intriguing to observe that either full-length or cytoplasmic portions of Met is present in the nucleus of different cellular contexts [20, 21]. Mechanisms underlying the translocation of Met from the cell surface to the nucleus have been suggested. Nuclear translocation of full-length Met has

been induced by HGF [21] while the identification of nuclear localization signal (NLS) in the cytoplasmic fragment of Met supports its entry into the nucleus [22]. Functionally, it has been shown that nMet possesses potential transcriptional activity in MDA-MB231 breast carcinoma cell and initiates calcium signals in SkHep1 cells [20, 21]. A recent paper shows that nMet upregulates SOX9 and activates β-catenin in prostate cancer cells [23]. These findings suggest that in addition to receiving and transducing extracellular signals as a receptor, Met exhibits unexplored capacities in the nucleus. In spite of the importance of Met as the promising therapeutic target in human cancers, the role of nMet in cancers deserves thorough investigation.

In human hepatocellular carcinoma (HCC), Met expression level is higher at both the mRNA and protein level when compared to normal or adjacent non-tumorous liver tissues [24]. Overexpression of Met has been shown to associate with metastasis, invasion and poor prognosis [25, 26]. Functional studies have shown that inhibition of Met activity and expression suppresses HCC cell migration and invasion [27, 28]. Recently, microRNAs have been shown to negatively regulate HCC cell motility by downregulating Met [29, 30]. When Met is co-expressed with c-Myc, hepatocyte proliferation is enhanced and c-Myc-induced tumorigenesis is greatly accelerated [31]. As demonstrated in transgenic mouse model, Met overexpressing hepatocytes readily develop HCC [32]. Another mouse model has shown that expression of the cytoplasmic portion of Met in mouse livers confers resistance to apoptosis [33]. On the contrary, hepatocytes in c-Met conditional knockout mice displayed an enhanced susceptibility to N-nitrosodiethylamine-induced hepatocarcinogenesis when compared to those in control mice [34]. These studies suggest that effects of Met may vary in different stages of carcinogenesis. Although Met has been well documented in HCC, the presence of nMet has not been reported. In the study, we show for the first time the presence and clinical significance of nMet in HCC.

Using different functional assays, nMet was demonstrated to promote HCC cell growth, migration, invasiveness in cell culture model as well as tumorigenesis and distant metastasis in animals. Mechanistically, nMet activates transforming growth factor beta-activated kinase 1 (TAK1) / nuclear factor kappa B (NF-κB) signaling pathway. Perturbation of TAK1/NF-κB pathway abrogates the promoting potential of nMet in HCC. Our study reveal nMet may represent a novel biomarker in HCC and targeting nMet signaling pathway suggests a new therapeutic approach for this aggressive disease.

2. Materials and Methods

2.1. Cell culture, transfection and stable cell lines

Human HCC cell lines, BEL7402 and SMMC7721 were obtained from Shanghai Institute of Cell Biology, Chinese Academy of Sciences, People's Republic of China (PRC). Other HCC cell lines include HLE and PLC/PRF/5 ~~and~~ were purchased from American Type Culture Collection (ATCC, Manassas, VA, USA). Metastatic HCC cell lines, MHCCLM3 and MHCC97L were gifts from Fudan University, China. MIHA is an immortalized normal liver cell line and HEK293FT is a normal human embryonal kidney cell line, both were purchased from ATCC. Transfection was performed using either Lipofectamine 2000 (Invitrogen, Gaithersburg, MD, USA) or FuGENE®6 (Roche, Basel, Switzerland) transfection reagent. Lenti-X™ Tet-On® Advanced Inducible Expression System (Clontech, Mountain View, CA, USA) was employed to establish nMet overexpression stable cell lines. A series of N-terminally truncated form of Met, named D972, P1027 and L1157 were designed by PCR (forward primer: D972: 5'-CGGGATCCATGGATGCAAGAGTACACACTCC-3', P1027: 5'-CGGGATCCATGCCTCTGACAGACATGTCCCC-3', L1157: 5'-CGGGATCCATGCTACCATACATGAAACATGG-3'; reverse primer: 5'-CGAATTCTAAATCAGGCTACTGGGCCCAATC-3') using cDNA of the HCC cell line SMMC7221 as the template. A myc tag sequence was added into the expression vector pLVX-Tight-Puro (Clontech) before insertion of D972, P1027 and L1157. The pLVX-Tight-Puro-Myc-D972/P1027/L1157 was transfected into HEK293FT cell for lentivirus packaging. Virus was collected to infect HCC cell lines to establish the stable nMet expressing cell lines. Doxycycline (Clontech) was used to induce the expression of nMet. For TAK1 knockdown experiment,

shTAK1 expression clones were purchased from GeneCopoeia (Rockville, MD, USA).

2.2. Clinical samples and clinicopathological analysis

Paired samples of primary HCC and the corresponding non-tumorous liver tissues from 103 Chinese patients were obtained at the time of surgical resection at Queen Mary Hospital, Hong Kong. Use of human samples was approved by the Institutional Review Board of the University of Hong Kong/Hospital Authority Hong Kong West Cluster (HKU/HA HKW IRB). The association of nMet expression and clinicopathological parameters of the patients was analyzed by Chi-squared test (categorical data) and Mann-Whitney U test (nonparametric continuous data) wherever appropriate. The association of nMet expression with the patients' overall survival rate and disease-free survival rate was examined by Kaplan Meier method. All statistical analyses were performed by IBM SPSS Statistics 23 (SPSS Inc., Chicago, IL) as described. A *P*-value less than 0.05 ($P < 0.05$) is considered to be statistically significant.

2.3. Immunohistochemistry (IHC)

IHC was performed on formalin-fixed, paraffin-embedded liver tissues sections followed by Aperio ScanScope CS System processing. High-quality digital images were created for analysis. The overall intensity of nuclear staining was graded. To determine the percentage of nuclei with positive Met staining, nuclear quantification was performed by the Aperio SlideAnalysis™Toolbox.

2.4. Cell proliferation and soft agar assay

Proliferation rate of adherent cells was determined by BrdU (bromodeoxyuridine) incorporation.

Cells were seeded in a 96-well plate and subjected to BrdU incorporation assay (Roche) according to manufacturer's instructions. Photometric detection was performed in Infinite® F200 microplate reader (Tecan, Maennedorf, Switzerland). Anchorage independent growth of cells was assessed by soft agar assay. The number and size of colonies were evaluated under light microscope. Detailed procedures are described elsewhere.

2.5. Cell migration and invasion assay

Transwell® Permeable Supports (inserts of 6.5 mm in diameter) (Corning, NY, USA) were used for cell migration assay. For cell invasion assay, Transwell® Permeable Supports inserts were coated with BD Matrigel™ Basement Membrane Matrix (BD Bioscience, Beillerica, MA, USA). Cell suspension in serum-free medium was added to the upper chamber at various densities depending on the cell line. Detailed procedures are described elsewhere.

2.6. Subcutaneous injection and orthotopic liver implantation

To perform subcutaneous injection, HCC cells were inoculated into the right flank of male 5-week old BALB/c nude mice. At the end of experiment, tumors were excised and weighed. Tumor seed obtained from subcutaneous injection was used for orthotopic implantation in male BALB/C nude mice. Mice were anesthetized and laparotomy was performed to expose the liver, and the tumor cube was inserted into the liver capsule using a needle. The mice with implanted tumors, which were derived from a luciferase-labeled cell line, were subjected to weekly bioluminescent imaging. Mice were anesthetized and injected with D-luciferin (Xenogen, Hopkinton, MA, USA) before imaging. Images were captured and the bioluminescent signal was quantified using IVIS 100 Imaging System (Xenogen). At the end of experiment, the mice were

sacrificed and their lungs and livers were excised for histological analysis. Animals (Control of Experiments) Ordinance (Hong Kong) and animal experimentation guidance from The University of Hong Kong were strictly followed for all animal work performed.

2.7. Statistical analysis

One-way ANOVA, performed by GraphPad Prism 5 (San Diego, CA, USA), was used for statistical analyses in various functional assays in this study. Clinicopathological analysis was analyzed with Fisher's exact test using IBM SPSS 23 for Windows. A *P*-value less than 0.05 was considered as statistically significant.

Additional experimental procedures are provided in the Supplementary Material and Methods.

3. Results

3.1. nMet was frequently overexpressed and associated with aggressive clinical features and poor prognosis in HCC

Anti-Met antibodies C28, raised against the C-terminal cytoplasmic domain of Met, and EP1454Y, raised against the N-terminal domain of Met, were used to detect ~~the nuclear and cytoplasmic~~ Met expression in the nucleus and cytoplasm in HCC tissue samples~~, respectively~~. EP1454Y antibody detected cytoplasmic expression while C28 antibody revealed both cytoplasmic and intense nuclear stain (Fig. 1A). In 89.3% (92/103) of the paired HCC samples, nMet staining was stronger in tumorous tissues when compared to the corresponding non-tumorous liver tissues (Fig. 1B). The percentage of nuclei with positive Met staining was significantly higher in tumorous tissues (range: 1.48 - 74.89%) than non-tumorous tissues (range: 3.61 - 40.8%) (Fig. 1C; $P < 0.001$; Mann-Whitney U test). nMet expression increased progressively along HCC development (Fig. 1D), with significant increase from the progression of cirrhotic liver (median: 18.19%) to early stage HCC (median: 32.15%) ($P < 0.001$; Mann-Whitney U test), as well as from early to advanced stage HCC (median: 42.71%) ($P < 0.05$; Mann-Whitney U test). A cutoff point was made to segregate the tumorous samples into low (35 cases; range: 1.48 - 33.31%) and high (68 cases; range: 33.32 - 74.89%) percentage of nMet groups. The higher level of nMet was significantly associated with cirrhosis ($P = 0.031$; Chi-squared test), poorer cellular differentiation ($P = 0.019$; Chi-squared test), presence of venous invasion ($P = 0.037$; Chi-squared test), as well as advanced HCC with pTMN stages III-IV ($P = 0.002$; Chi-squared test) (Table 1). Additionally, an association was observed between higher

nMet level and poorer overall survival ($P < 0.05$, log-rank test)~~, as shown in the Kaplan Meier plot~~ (Fig. 1E) but not correlated with disease-free survival (data not shown). ~~-~~

3.2. nMet comprised the carboxyl terminus of Met

Expression and subcellular localization of Met was examined in a non-tumorigenic liver cell line MIHA, non-metastatic HCC cell lines PLC/PRF/5, SMMC7221 and HLE, as well as the metastatic HCC cell lines MHCCLM3 and MHCC97L. A band size of around 50-kDa was revealed by C28 antibody but not EP1454 antibody in all HCC cell lines except MIHA, suggesting the protein size of nMet (Fig. 2A). Cellular fractionation revealed that a 48-kDa Met was detected in the total cell lysate as well as the nuclear fraction of BEL7402 and SMMC7221 cells (Fig. 2B), evidently indicating the presence of nMet in HCC cell lines. HGF, the native ligand of Met, did not affect nMet expression. Moreover, phospho-Met antibody detected strong signal of full-length Met but not nMet, suggesting nMet is not phosphorylated under HGF treatment (Fig. 2C). Using immunofluorescence microscopy, membranous and cytoplasmic Met was detected by EP1454Y while, membranous, cytoplasmic as well as nuclear staining was revealed by C28 (Fig. 2D). nMet was also detected in other HCC cells including PLC, HLE and SMMC7221 (Fig. 2E). To examine whether HGF affects the subcellular localization of nMet, we expressed GFP-tagged constructs expressing cytoplasmic fragment of Met (D972, P1027 and L1157). The immunofluorescent staining showed that the nuclear translocation of Met was HGF independent (Supplementary Fig. 1A). RTKs have been shown to shuttle between membrane and nucleus. However, treatment of cells with Leptomycin B (LMB), an inhibitor of CRM1 nuclear exporter, showed that nMet remained static in the nucleus (Supplementary Fig. 1B).

3.3. nMet exerted its functional effect in the nucleus to promote cell proliferation, anchorage independent growth and in vivo tumorigenicity

Based on the size of Met fragment observed in the nuclear lysates of HCC cells (Fig. 2), fragments of Met cytoplasmic fragments were constructed to be expressed in HCC cells for functional characterization (Supplementary Fig. 2A and 2B). Stable inducible clones of nMet were established in SMMC7721 and BEL7402 cells. The expressions of D972, P1027 and L1157 Met cytoplasmic fragments were induced by doxycycline in a time and dosage dependent manner (Supplementary Fig. 2C and 2D). Immunofluorescent staining and cellular fractionation revealed that D972 and P1027 were expressed in the nucleus while L1157 was only detected in the cytoplasm (Supplementary Fig. 3).

BrdU incorporation assay and soft agar assays were performed to study the effect of Met cytoplasmic fragments in HCC cells. Compared with the vector control cells, only D972 significantly promoted cell proliferation (SMMC7721, $P < 0.01$; BEL7402, $P < 0.001$) and anchorage independent growth (SMMC7721, $P < 0.01$; BEL7402, $P < 0.001$) (Supplementary Fig. 4C and 4D). These functional analyses demonstrated that Met cytoplasmic fragments only exerted functional effect when they were expressed in the nucleus. In order to confirm the promoting effect ~~of~~ was due to the induced expression of D972, BrdU incorporation assay and soft agar assays were performed ~~in~~ on ~~cells~~ D972 cells established in SMMC7721 and BEL7402 cells treated with or without doxycycline (Fig. 34A). The results revealed that ~~in both HCC ,~~ only D972 cells treated with doxycycline showed enhancement in cell proliferation and anchorage independent growth (Fig. 3B and 3-C).

In ~~nude mice assay~~xenograft experiment, BEL7402 D972 cells efficiently promoted tumor formation and resulted in bigger tumors than the vector control ($P < 0.05$) (Fig. 3D).

Similar findings were observed in SMMC7721 D972 cells (Supplementary Fig. 5A and 5B). In another experiment, development of tumor ~~development of~~ derived from SMMC7721 D972 cells was compared in mice fed with or without doxycycline-containing drinking water. The result showed that larger tumors were formed in mice treated with doxycycline (Supplementary Fig. 5C). This data provided evidence that the promoting effect in tumor formation was due to the doxycycline-induced expression of D972. Solid tumors derived from BEL7402 D972 and control cells in the subcutaneous injection were subjected to orthotopic liver implantation to reveal the growth of tumors in liver. Five weeks after implantation, luciferase imaging revealed a more prominent signal in mice implanted with tumors of D972 when compared to the vector control mice (Fig. 3~~5~~E). Bigger tumors were found in the liver of D972 group. Tumors of D972 group displayed an invasive growth front by invading adjacent liver tissues. However, such aggressive features were not seen in the tumors of the control group.

3.4. nMet enhanced HCC cell migration, invasiveness and metastasis

Expression of nMet significantly correlated with tumor invasion; a clinical feature of cancer metastasis. This result prompted us to further investigate the functional effect of nMet in HCC cell motility. Consistent with the promoting effect of nMet in cell growth, only D972, but not P1027 and L1157, significantly promoted cell migration (SMMC7721, BEL7402, $P < 0.05$) and cell invasiveness (SMMC7721, $P < 0.001$; BEL7402, $P < 0.01$) (Supplementary Fig. 4E and 4F). ~~The promoting effect of nMet in~~Enhancement in cell migration and invasiveness was only evident in D972 cells treated with doxycycline (Figure 4A and 4~~-~~B). Subsequently, we examined the role of nMet in HCC metastasis by establishing cells with doxycycline-inducible expression of D972, P1027 and L1157 Met cytoplasmic fragments ~~nMet~~ in a metastatic HCC cell line,

MHCC97L ~~cells~~ (Fig. 4C; Supplementary Fig. 6). Similarly, only D972 exerted effect in promoting cell migration and invasion (Supplementary Fig. 7). To examine the effect of D972 in metastasis, tumor seed derived from MHCC97L D972 and control cells were implanted into liver of mice. Five weeks post implantation, bioluminescence imaging revealed stronger luciferase signal in animals implanted with D972 tumor seed than the control group (Fig. 4D). Consistently, larger liver tumor size was detected in D972 group. The growth fronts of D972 tumors were irregular and invasive, whereas the tumor growth fronts of the control group were found to be bulging and less invasive. The expression of D972 in the tumors was confirmed by immunohistochemistry (Fig. 4E). Moreover, distant lung metastasis and metastatic tumor foci were only observed in lung tissues of D972 group but not in the control group (Fig. 4F).

3.5. nMet activated TAK1/NF-κB pathway

In order to interrogate the molecular mechanism mediated by nMet, various luciferase-conjugated reporters were examined for their activation by Met fragments (Supplementary Fig. 8A). Among all the reporters, D972 could robustly activate NF-κB reporter ($P < 0.001$) (Fig. 5A, Supplementary Fig. 8B). Levels of p-IKKα/β and nuclear p-p65 were higher in BEL7402 D972 stable clone than in the control vector clone (Fig. 5B). We next explored the possibility about the activation of TAK1 by D972. In the stable clone of D972, both TAK1 mRNA and protein levels were upregulated (Fig. 5C). Luciferase reporter carrying TAK1 promoter displayed a higher luciferase activity in D972 cells than in vector control cells (Fig. 5D). To examine whether nMet mediates its functional effects indeed through the activation of TAK1/NF-κB pathway, functional assays of D972 stable clones were performed when NF-κB pathway was perturbed. Treatment of BEL7402 D972 stable clones with IMD-0354, an inhibitor of IKKβ, lowered the

expression of p-IKKα/β and the migratory ($P < 0.05$) and invasive ($P < 0.001$) potentials of cells (Fig. 5E~~D~~). In addition, knockdown of p65 expression in D972 stable clone reduced cell migration ($P < 0.001$) and invasiveness ($P < 0.05$) (Fig. 5F~~E~~).

To investigate whether the functional effect of nMet is driven by TAK1, TAK1 stable knockdown clones (shTAK1#32 and shTAK#34) were established in MHCC97L D972 cells. Suppression of TAK1 in MHCC97L D972 cells concomitantly reduced the expression of p-p65 (Fig. 6A). TAK1 knockdown stable clones showed reduced cell migration (shTAK1#32, shTAK1#34, $P < 0.001$) and invasion (shTAK1#32, shTAK1#34, $P < 0.001$) (Fig. 6B). In ~~nude mice assay~~xenograft experiment, TAK1 knockdown stable clones exhibited slower tumor growth (shTAK1#32, shTAK1#34, $P < 0.001$) and formed smaller tumors (shTAK1#32, shTAK1#34, $P < 0.001$) as compared to non-target control clones (Fig. 6C; Supplementary Fig. 9). IHC staining revealed reduced expressions of TAK1 and p-p65 expressions in excised tumors derived from TAK1 knockdown stable cells (Fig. 6D). Furthermore, potential of TAK1 knockdown stable cells in distant metastasis was studied using orthotopic liver implantation. Five weeks post implantation, smaller liver tumors were found in mice implanted with seed derived from TAK1 knockdown cells (shTAK1#32, $P < 0.001$; shTAK1#34, $P < 0.01$) (Fig. 6E). Histological examination of the livers revealed that tumors of TAK1 knockdown stable clones displayed a less invasive growth front than the tumors in the control group. Moreover, lungs of animals in knockdown group showed no distant metastases. Metastatic tumor foci were only observed in lung tissues of non-target control group (Fig. 6F).

4. Discussion

Aberrant expression and activation of HGF/Met signaling pathway are frequently found in human cancers which make Met an attractive therapeutic target for human cancers. Currently, therapeutic monoclonal antibodies against HGF and Met, as well as small molecule inhibitors antagonizing the kinase activity of Met, are in different phases of clinical trials [35]. The existence and potential functions of Met in the nucleus intelligibly challenge the current therapeutic strategies against Met surface receptor. This situation provides a compelling rationale for obtaining a better understanding about the spatial distribution and roles of Met in different subcellular compartments.

Met localization is not restricted to the cell membrane and cytoplasm. In fact, Met can also be detected in the nucleus. nMet was first observed in melanoma tumors and cell lines independent of HGF [10]. However, Met levels in the nuclei of uveal melanomas and metastatic breast cancer cells are found to be enhanced by HGF stimulation [15, 36]. nMet is also detected in various cancer cell lines [18, 20] and cancerous tissues, particularly at the invasive front [11], suggesting its potential role in human cancers. Interestingly, the distribution pattern of Met is not stagnant. Nuclear translocation of Met may occur in rapidly dividing and not fully differentiated cells [14]. Using antibodies against the carboxyl and amino termini of Met, different outcomes have been observed. Met expression detected by antibodies against the carboxyl terminus of Met is significantly correlated with a poor prognosis in lymph node-negative breast carcinomas. Intriguingly, such correlation is not observed when antibodies targeting the amino terminus of Met are used [12]. Consistent with the reported study, we observed strong nuclear staining in HCC tissues using C28 antibody that directs against the C-terminal of Met (immunogen

sequence: P1366-S1390) whereas EP1454Y antibody, which directs against the extracellular domain of Met, failed to detect such nuclear pattern of Met. Our findings on nMet expression suggest that nMet plays an indispensable role in HCC progression and could be a potential prognostic marker for HCC.

Regardless of the presence of HGF, a 60-kDa fragment of Met that localizes in the nucleus of epidermoid carcinoma cell line is recognized by antibodies against the carboxyl terminus of Met [14]. Due to the absence of a shorter transcript of Met in Northern blot analysis, this study postulates that nMet possibly results from the proteolytic cleavage of full-length Met receptor. In fact, nuclear and cytoplasmic Met of 75 kDa and 85 kDa have been detected in prostate cancer and musculoskeletal tumors, respectively. These observations implicate that the protein size of truncated Met may vary in different cell types. We observed nMet as a 50-kDa protein in various HCC cell lines of different metastatic potentials using C28 antibody. To exclude the possibility that the 50-kDa band is a cross-reacting protein, C12 antibody, which also targets the cytoplasmic domain of Met (immunogen sequence: V1379-S1390), is used to detect proteins immunoprecipitated by C28 antibody. C12 antibody successfully revealed positive signal with the same molecular weight in the nuclear and total cell lysates of HCC cells. Using the same C12 antibody, Met is detected in the nuclear lysate of oral squamous cell carcinoma [18].

Several RTKs are processed by sequential proteolysis which includes shedding of ectodomain by ADAM family of metalloproteinases, followed by cleavage within the transmembrane domain by γ-secretase/presenilin-1/2 [37]. Indeed, ectodomain shedding of Met is specifically inhibited by the tissue inhibitor of metalloproteinase, TIMP-3 [38]. Treatment with γ-secretase inhibitor reduces the accumulation of nMet in prostate cancer cells [23]. In plasma

and urine samples from mice implanted with human tumor xenografts, Met ectodomain fragments are detected. More importantly, the level of soluble Met directly correlates with the tumor volume [39]. In patients with uveal melanoma, higher serum level of soluble Met is found in patients with metastatic disease than those with no sign of metastasis [40]. These findings point to the significance of proteolytic cleavage of Met in cancers. Upon HGF binding, Met has been shown to be internalized and degraded via the formation of endophilin-CIN85-Cbl complex [41]. Proteolytic processing acts as a negative regulatory mechanism to prevent oversignaling of Met; yet it is complicated by the generation of biologically active cytoplasmic fragments of Met. An intracellular 40-kDa fragment, resulted from caspase cleavage of Met, induces apoptosis under stress [42]. Downregulation of Met by presenilin-dependent regulated intramembrane proteolysis also leads to the generation of small labile fragments of Met [43]. Whether and how these cleaved fragments translocate into the nucleus remain to be answered. The nuclear translocation of the cytoplasmic Met fragment has been shown to be regulated by the WW domain-containing oxidoreductase (Wwox) tumor suppressor [20]. Nevertheless, HGF induces nuclear translocation of the full-length Met receptor in a manner that is dependent on the adaptor proteins Gab1 and importin β1 [21]. NLS mediates the translocation of protein molecules larger than 30-40-kDa from the cytoplasm to the nucleus. A recent study mapped a NLS in the juxtamembrane region of Met (H1068-H1079) [22]. This pH-dependent NLS coupled with importin β1 answered the query on how the cytoplasmic fragment of Met can dislocate into the nucleus. We observed that D972 and P1027 but not L1157 localize in the nucleus of HCC cells, suggesting that the region between P1027 and L1157 is responsible for the nuclear translocation of Met. This defined region, which coincides with the location of NLS identified in the previous

study, further supports the NLS-dependent mechanism for directing Met into the nucleus in HCC cells.

Despite the presence of nMet has been reported, its functions remain obscure. Predominant expression of phospho-Met (pMet) in the nucleus of cancerous tissues and cell lines is suggestive that nMet is active [13, 16]. pMet colocalizes with PAX5 transcription factor upon HGF treatment, implying the potential transcriptional activity of nMet [16]. In this perspective, transactivating activity of nMet is further supported by the ability of Met-Gal4 DNA-binding domain fusion protein to transactivate Gal4-luciferase reporter [20]. In our study, doxycycline-induced expression of nMet elevates the transcription of TAK1. However, whether nMet activates TAK1 promoter in a direct or an indirect fashion needs to be further investigated. In our study, P1027 fragment although localizes in the nucleus did not induce similar biological effects as D972 fragment. We suspect that the truncated region of P1072 might affect the biochemical property of nMet. Besides the transactivating activity, nMet has been shown to interact with SMC-1, a chromosome-associated protein, further supports the undefined functional role of Met in the nucleus [44].

Our study discovered a novel mechanism by which nMet mediates the activation of TAK1/NF-κB pathway to drive HCC tumorigenesis and metastasis. nMet overexpression promotes the transcription of TAK1 resulting in the enhanced level of TAK1. Elevated level of TAK1 phosphorylates IKKβ, leading to IκBα phosphorylation and its subsequent proteasomal degradation. Released NF-κB then translocates to the nucleus where it induces transcription of pro-metastatic genes to promote HCC cell migration, invasion and metastasis (Fig. 7). In accordance with the oncogenic role of nMet that we observed in functional studies, nMet overexpression is significantly correlated with HCC patients with advanced tumor stage and

venous invasion, an indication of metastasis (Table 1). TAK1 is an intracellular serine/threonine kinase that regulates both NF-κB and mitogen-activated protein kinase (MAPK) signaling pathways involved in diverse biological processes [45]. TAK1 play a dual role in tumor initiation, progression and metastasis. Disruption of TAK1 in hepatocytes causes hepatic injury, inflammation, fibrosis, and carcinogenesis [46]. Suppression of TAK1 also promotes prostate tumorigenesis [47]. Nevertheless, inhibition of TAK1 prevents lung metastasis of breast cancer [48]. Through the activation of NF-κB signaling, TAK1 enhances the oncogenic capacity of ovarian cancer cells [49]. In one study, HGF has been shown to activate Src leading to the stimulation of NF-κB through TAK1, suggesting that Met as a receptor of HGF is involved in Src-mediated activation of TAK1/NF-κB pathway [50]. Here, we delineate a novel mechanistic pathway showing the connection of nMet and TAK1/NF-κB pathway leading to the progression of HCC.

In this study, we have provided the first evidence about the presence of nMet in HCC which has profound prognostic value. Our findings have also derived new mechanistic insights into hepatocarcinogenesis. More importantly, the expanding knowledge on the signaling networks and actions of Met in the nucleus will provide important insights into the development of therapeutic strategies against aberrant Met in human cancers.

Acknowledgements

We thank the Faculty of Medicine Core Facility for providing Xenogen imaging service for our animal experimentation.

Funding

This work was supported by the Hong Kong Research Grants Council [HKU783613M]; The University of Hong Kong Seed Funding Programme for Basic Research [20111115902] and [201011159041].

Conflicts of interest

The authors declare no potential conflicts of interest.

References

[1] C. Ponzetto, A. Bardelli, Z. Zhen, F. Maina, P. dalla Zonca, S. Giordano, et al. A multifunctional docking site mediates signaling and transformation by the hepatocyte growth factor/scatter factor receptor family. Cell 77 (1994) 261-271.

[2] Y. Uehara, O. Minowa, C. Mori, K. Shiota, J. Kuno, T. Noda, et al. Placental defect and embryonic lethality in mice lacking hepatocyte growth factor/scatter factor. Nature 373 (1995) 702-705.

[3] F. Maina, M.C. Hilton, C. Ponzetto, A.M. Davies, R. Klein. Met receptor signaling is required for sensory nerve development and HGF promotes axonal growth and survival of sensory neurons. Genes Dev 11 (1997) 3341-3350.

[4] J. Chmielowiec, M. Borowiak, M. Morkel, T. Stradal, B. Munz, S. Werner, et al. c-Met is essential for wound healing in the skin. J Cell Biol 177 (2007) 151-162.

[5] M. Borowiak, A.N. Garratt, T. Wustefeld, M. Strehle, C. Trautwein, C. Birchmeier. Met provides essential signals for liver regeneration. Proc Natl Acad Sci U S A 101 (2004) 10608-10613.

[6] C. Birchmeier, W. Birchmeier, E. Gherardi, G.F. Vande Woude. Met, metastasis, motility and more. Nat Rev Mol Cell Biol 4 (2003) 915-925.

[7] C.Y. Ni, M.P. Murphy, T.E. Golde, G. Carpenter. gamma -Secretase cleavage and nuclear localization of ErbB-4 receptor tyrosine kinase. Science 294 (2001) 2179-2181.

[8] S.Y. Lin, K. Makino, W. Xia, A. Matin, Y. Wen, K.Y. Kwong, et al. Nuclear localization of EGF receptor and its potential new role as a transcription factor. Nat Cell Biol 3 (2001) 802-808.

Formatted: Line spacing: Double

Field Code Changed

[9] G. Carpenter. Nuclear localization and possible functions of receptor tyrosine kinases. Curr Opin Cell Biol 15 (2003) 143-148.

[10] K. Saitoh, H. Takahashi, N. Sawada, P.G. Parsons. Detection of the c-met proto-oncogene product in normal skin and tumours of melanocytic origin. J Pathol 174 (1994) 191-199.

[11] G. Edakuni, E. Sasatomi, T. Satoh, O. Tokunaga, K. Miyazaki. Expression of the hepatocyte growth factor/c-Met pathway is increased at the cancer front in breast carcinoma. Pathol Int 51 (2001) 172-178.

[12] J.Y. Kang, M. Dolled-Filhart, I.T. Ocal, B. Singh, C.Y. Lin, R.B. Dickson, et al. Tissue microarray analysis of hepatocyte growth factor/Met pathway components reveals a role for Met, matriptase, and hepatocyte growth factor activator inhibitor 1 in the progression of node-negative breast cancer. Cancer Res 63 (2003) 1101-1105.

[13] P.C. Ma, R. Jagadeeswaran, S. Jagadeesh, M.S. Tretiakova, V. Nallasura, E.A. Fox, et al. Functional expression and mutations of c-Met and its therapeutic inhibition with SU11274 and small interfering RNA in non-small cell lung cancer. Cancer Res 65 (2005) 1479-1488.

[14] S. Pozner-Moulis, D.J. Pappas, D.L. Rimm. Met, the hepatocyte growth factor receptor, localizes to the nucleus in cells at low density. Cancer Res 66 (2006) 7976-7982.

[15] M. Ye, D. Hu, L. Tu, X. Zhou, F. Lu, B. Wen, et al. Involvement of PI3K/Akt signaling pathway in hepatocyte growth factor-induced migration of uveal melanoma cells. Invest Ophthalmol Vis Sci 49 (2008) 497-504.

[16] R. Kanteti, V. Nallasura, S. Loganathan, M. Tretiakova, T. Kroll, S. Krishnaswamy, et al. PAX5 is expressed in small-cell lung cancer and positively regulates c-Met transcription. Lab Invest 89 (2009) 301-314.

[17] Y.S. Chen, J.T. Wang, Y.F. Chang, B.Y. Liu, Y.P. Wang, A. Sun, et al. Expression of hepatocyte growth factor and c-met protein is significantly associated with the progression of oral squamous cell carcinoma in Taiwan. J Oral Pathol Med 33 (2004) 209-217.

[18] I.J. Brusevold, T.M. Soland, C. Khuu, T. Christoffersen, M. Bryne. Nuclear and cytoplasmic expression of Met in oral squamous cell carcinoma and in an organotypic oral cancer model. Eur J Oral Sci 118 (2010) 342-349.

[19] S. Pozner-Moulis, M. Cregger, R.L. Camp, D.L. Rimm. Antibody validation by quantitative analysis of protein expression using expression of Met in breast cancer as a model. Lab Invest 87 (2007) 251-260.

[20] E. Matteucci, P. Bendinelli, M.A. Desiderio. Nuclear localization of active HGF receptor Met in aggressive MDA-MB231 breast carcinoma cells. Carcinogenesis 30 (2009) 937-945.

[21] D.A. Gomes, M.A. Rodrigues, M.F. Leite, M.V. Gomez, P. Varnai, T. Balla, et al. c-Met must translocate to the nucleus to initiate calcium signals. J Biol Chem 283 (2008) 4344-4351.

[22] S.C. Chaudhary, M.G. Cho, T.T. Nguyen, K.S. Park, M.H. Kwon, J.H. Lee. A putative pH-dependent nuclear localization signal in the juxtamembrane region of c-Met. Exp Mol Med 46 (2014) e119.

[23] Y. Xie, W. Lu, S. Liu, Q. Yang, B.S. Carver, E. Li, et al. Crosstalk between nuclear MET and SOX9/beta-catenin correlates with castration-resistant prostate cancer. Mol Endocrinol 28 (2014) 1629-1639.

[24] J.J. Gao, Y. Inagaki, X. Xue, X.J. Qu, W. Tang. c-Met: A potential therapeutic target for hepatocellular carcinoma. Drug Discov Ther 5 (2011) 2-11.

[25] P. Kaposi-Novak, J.S. Lee, L. Gomez-Quiroz, C. Coulouarn, V.M. Factor, S.S. Thorgeirsson. Met-regulated expression signature defines a subset of human hepatocellular carcinomas with poor prognosis and aggressive phenotype. J Clin Invest 116 (2006) 1582-1595.

[26] A.W. Ke, G.M. Shi, J. Zhou, F.Z. Wu, Z.B. Ding, M.Y. Hu, et al. Role of overexpression of CD151 and/or c-Met in predicting prognosis of hepatocellular carcinoma. Hepatology 49 (2009) 491-503.

[27] H. You, W. Ding, H. Dang, Y. Jiang, C.B. Rountree. c-Met represents a potential therapeutic target for personalized treatment in hepatocellular carcinoma. Hepatology 54 (2011) 879-889.

[28] A. Salvi, B. Arici, N. Portolani, S.M. Giulini, G. De Petro, S. Barlati. In vitro c-met inhibition by antisense RNA and plasmid-based RNAi down-modulates migration and invasion of hepatocellular carcinoma cells. Int J Oncol 31 (2007) 451-460.

[29] N. Li, H. Fu, Y. Tie, Z. Hu, W. Kong, Y. Wu, et al. miR-34a inhibits migration and invasion by down-regulation of c-Met expression in human hepatocellular carcinoma cells. Cancer Lett 275 (2009) 44-53.

[30] A. Salvi, C. Sabelli, S. Moncini, M. Venturin, B. Arici, P. Riva, et al. MicroRNA-23b mediates urokinase and c-met downmodulation and a decreased migration of human hepatocellular carcinoma cells. FEBS J 276 (2009) 2966-2982.

[31] L. Amicone, O. Terradillos, L. Calvo, B. Costabile, C. Cicchini, C. Della Rocca, et al. Synergy between truncated c-Met (cyto-Met) and c-Myc in liver oncogenesis: importance of TGF-beta signalling in the control of liver homeostasis and transformation. Oncogene 21 (2002) 1335-1345.

[32] R. Wang, L.D. Ferrell, S. Faouzi, J.J. Maher, J.M. Bishop. Activation of the Met receptor by cell attachment induces and sustains hepatocellular carcinomas in transgenic mice. J Cell Biol 153 (2001) 1023-1034.

[33] L. Amicone, F.M. Spagnoli, G. Spath, S. Giordano, C. Tommasini, S. Bernardini, et al. Transgenic expression in the liver of truncated Met blocks apoptosis and permits immortalization of hepatocytes. EMBO J 16 (1997) 495-503.

[34] T. Takami, P. Kaposi-Novak, K. Uchida, L.E. Gomez-Quiroz, E.A. Conner, V.M. Factor, et al. Loss of hepatocyte growth factor/c-Met signaling pathway accelerates early stages of N-nitrosodiethylamine induced hepatocarcinogenesis. Cancer Res 67 (2007) 9844-9851.

[35] A. Furlan, Z. Kherrouche, R. Montagne, M.C. Copin, D. Tulasne. Thirty years of research on met receptor to move a biomarker from bench to bedside. Cancer Res 74 (2014) 6737-6744.

[36] S. Previdi, P. Maroni, E. Matteucci, M. Broggini, P. Bendinelli, M.A. Desiderio. Interaction between human-breast cancer metastasis and bone microenvironment through activated hepatocyte growth factor/Met and beta-catenin/Wnt pathways. Eur J Cancer 46 (2010) 1679-1691.

[37] G. Carpenter, H.J. Liao. Trafficking of receptor tyrosine kinases to the nucleus. Exp Cell Res 315 (2009) 1556-1566.

[38] D. Nath, N.J. Williamson, R. Jarvis, G. Murphy. Shedding of c-Met is regulated by crosstalk between a G-protein coupled receptor and the EGF receptor and is mediated by a TIMP-3 sensitive metalloproteinase. J Cell Sci 114 (2001) 1213-1220.

[39] G. Athauda, A. Giubellino, J.A. Coleman, C. Horak, P.S. Steeg, M.J. Lee, et al. c-Met ectodomain shedding rate correlates with malignant potential. Clin Cancer Res 12 (2006) 4154-4162.

[40] G. Barisione, M. Fabbi, A. Gino, P. Queirolo, L. Orgiano, L. Spano, et al. Potential Role of Soluble c-Met as a New Candidate Biomarker of Metastatic Uveal Melanoma. JAMA Ophthalmol 133 (2015) 1013-1021.

[41] A. Petrelli, G.F. Gilestro, S. Lanzardo, P.M. Comoglio, N. Migone, S. Giordano. The endophilin-CIN85-Cbl complex mediates ligand-dependent downregulation of c-Met. Nature 416 (2002) 187-190.

[42] B. Foveau, C. Leroy, F. Ancot, J. Deheuninck, Z. Ji, V. Fafeur, et al. Amplification of apoptosis through sequential caspase cleavage of the MET tyrosine kinase receptor. Cell Death Differ 14 (2007) 752-764.

[43] B. Foveau, F. Ancot, C. Leroy, A. Petrelli, K. Reiss, V. Vingtdeux, et al. Down-regulation of the met receptor tyrosine kinase by presenilin-dependent regulated intramembrane proteolysis. Mol Biol Cell 20 (2009) 2495-2507.

[44] C.P. Schaaf, J. Benzing, T. Schmitt, D.H. Erz, M. Tewes, C.R. Bartram, et al. Novel interaction partners of the TPR/MET tyrosine kinase. FASEB J 19 (2005) 267-269.

[45] Y.S. Roh, J. Song, E. Seki. TAK1 regulates hepatic cell survival and carcinogenesis. J Gastroenterol 49 (2014) 185-194.

[46] S. Inokuchi, T. Aoyama, K. Miura, C.H. Osterreicher, Y. Kodama, K. Miyai, et al. Disruption of TAK1 in hepatocytes causes hepatic injury, inflammation, fibrosis, and carcinogenesis. Proc Natl Acad Sci U S A 107 (2010) 844-849.

[47] M. Wu, L. Shi, A. Cimic, L. Romero, G. Sui, C.J. Lees, et al. Suppression of Tak1 promotes prostate tumorigenesis. Cancer Res 72 (2012) 2833-2843.

[48] D.M. Ray, P.H. Myers, J.T. Painter, M.J. Hoenerhoff, K. Olden, J.D. Roberts. Inhibition of transforming growth factor-beta-activated kinase-1 blocks cancer cell adhesion, invasion, and metastasis. Br J Cancer 107 (2012) 129-136.

[49] P.C. Cai, L. Shi, V.W. Liu, H.W. Tang, I.J. Liu, T.H. Leung, et al. Elevated TAK1 augments tumor growth and metastatic capacities of ovarian cancer cells through activation of NF-kappaB signaling. Oncotarget 5 (2014) 7549-7562.

[50] S. Fan, Q. Meng, J.J. Laterra, E.M. Rosen. Role of Src signal transduction pathways in scatter factor-mediated cellular protection. J Biol Chem 284 (2009) 7561-7577.

Table 1. Clinicopathological correlation of nuclear Met expression in human HCC

	Low % (No. of cases)	High % (No. of cases)	*P* value
Sex			
Male	27	54	
Female	8	12	0.606
Age 13-74			
≤ 52 years	17	37	
>52 years	18	30	0.539
Non-tumorous liver status			
Normal	3	2	
Chronic hepatitis/cirrhosis	32	65	0.336
Cirrhosis status			
No cirrhosis	27	36	
Cirrhosis	8	31	0.031*
Tumor size			
≤ 5 cm	11	25	
> 5 cm	24	43	0.666
No. of tumour nodules			
1	31	52	
≥ 2	4	16	0.191
Tumor encapsulation			
Absent	24	45	
Present	9	20	0.817
Cellular differentiation[#]			
I-II	25	31	
III-IV	9	35	0.019*
pTMN stage			
I-II	20	17	
III-IV	14	49	0.002*
Hepatitis B surface antigen			
Absent	5	10	
Present	29	56	1.000
Venous Invasion			
Absent	21	25	
Present	14	42	0.037*
Tumor microsatellite formation			
Absent	19	28	
Present	16	39	0.296
Direct liver invasion[##]			
Absent	16	27	
Present	10	24	0.628

According to Edmondson grading
Invasion of tumor into the adjacent liver parenchyma
* $P < 0.05$

Figure legends

Figure 1.

nMet was overexpressed in HCCs. A, Representative HCC tissues showing differential staining pattern revealed by IHC using C28 and EP1454Y antibodies. Insets showing Met staining in membrane, cytoplasm and nucleus are included (Scale bar: 50 μm). B, An example ~~from~~ of HCC patient sample revealed stronger nuclear staining in tumorous (T) tissues than in the corresponding non-tumorous (NT) liver tissues detected by C28 antibody (Scale bar: 50 μm). Insets comparing the staining in the nucleus of T and NT tissues. C, nMet expression in 103 HCC clinical samples was detected by C28 antibody and was scored by the Aperio system. The overall nMet expression was significantly higher in tumorous (T) tissues than in the corresponding non-tumorous (NT) liver tissues. D, Progressive increase in nMet expression during HCC development from non-tumorous livers without cirrhosis (n = 61) and with cirrhosis (n = 39) to early HCC with pTMN stages I&II (n = 37) and advanced HCC with pTMN stages III&IV (n = 63). E, Cases with higher nMet expression had a poorer overall survival. *P*-value less than 0.05 is regarded as statistically significant.

Formatted: Font: Italic

Figure 2.

Expression and subcellular localization of Met in HCC cell lines. A, EP1454Y (EP) and C28 antibodies revealed different banding patterns of Met expression in HCC cell lines. Small band sizes of around 50-kDa were only detected by C28 in all HCC cell lines except MIHA, an immortalized liver cell line. B, Cellular fractionation revealed the presence of Met (48-kDa) in the nuclear fraction of BEL7402 and SMMC7721 cells. C, The 48-kDa band of Met was not

detected by phospho-Met (Y1234/1235) antibody under HGF stimulation. D, Immunofluorescence microscopy revealed that EP1454Y detected both cytoplasmic and membranous Met expression but not nuclear expression of Met, while C28 detected nuclear localization of Met in MHCC97L cells. E, C28 also detected nMet in PLC, HLE and SMMC7721 cells. Scale bar represents 10 μm.

Figure 3.

Doxycycline induced expression of D972 promoted in vitro HCC cell growth, anchorage independent growth and *in vivo* tumorigenesis. A, Expression of D972 in SMMC7721 and BEL7420 cells after 2 μg/ml of doxycycline (Dox) treatment for 24 hours was shown by western blotting. B, Induced expression of D972 upon doxycycline treatment significantly promoted cell proliferation when compared to D972 cells without doxycycline induction, as well as control cells treated with and without doxycycline. C, Induced expression of D972 significantly enhanced anchorage independent growth in SMMC7721 (*left*) and BEL7402 cells (*right*). Values of mean ± SD of triplicates were plotted. Three independent experiments were performed. D, Subcutaneous injection assay revealed that luciferase-labeled BEL7402 cells induced with D972 expression promoted tumor formation (n = 5 per group) (*left*). The overall weight of tumors of D972 group was significantly higher than that of the vector control group (*middle*). Immunohistochemistry staining confirmed the expression of induced nMet expression in D972 group but not in vector control group (*right*) (Magnification: 10×). E, Orthotopic liver implantation of tumor seed derived from BEL7402 D972 and control cells (n = 5 per group). Luciferase signal was higher in animals implanted with D972 tumor seed (*left*). Higher luciferase

signal was observed in the liver of D972 group (*middle*). H&E staining of liver tumors (*right*) (Magnification: 10×). Data with *P*-value less than 0.05 is considered as statistically significant.

Formatted: Font: Italic

Figure 4.

Doxycycline induced expression of D972 promoted HCC cell migration, invasiveness and metastasis. Induced expression of D972 promoted (A) cell migration and (B) cell invasiveness in SMMC7721 (*left*) and BEL7402 cells (*right*). Results are expressed as mean □ SD. Three independent experiments were performed. C, Stably transduced cells of metastatic MHCC97L were treated with 2 μg/ml Dox for 24 hours. Induced expression of Myc-tagged D972 was confirmed by western blot analysis using anti-Myc antibody. D, Orthotopic liver implantation of MHCC97L D972 clone resulted in stronger luciferase signal in animals implanted with tumor seed derived from D972 cells (*left*). D972 tumor seed formed significantly larger tumor in liver than the control tumor seed (n = 5 per group) (*middle* and *right*). E, H&E and immunohistochemistry staining of liver tumors (Magnification: 10×). F, Excised lung tissues showed higher incidence of distant metastases in animals implanted with D972 tumor seed than the control group (*left*). Lung metastasis evaluated according to the luciferase signal (*middle*). Lungs were excised and examined for metastatic foci by histological analysis. Representative images of H&E stained lung tissues (*right*) (Magnification: 10×). *P*-value less than 0.05 is regarded as statistically significant.

Formatted: Font: Italic

Figure 5.

D972 activated TAK1/NF-κB pathway. A, Expression constructs of D972 and NF-κB reporter were co-expressed in HEK293 cells. Luciferase activity was measured 24 hours post transfection.

D972 significantly activated NF-κB reporter. B, Higher nuclear p-p65 and p-IKKα/□ expressions were detected in the D972 stable clone when compared to the control stable clone. C, TAK1 expression in BEL7402 D972 stable clone was analyzed by western blotting and qPCR. D, Luciferase reporter carrying TAK1 promoter was expressed in MHCC97L vector and D972 cells and the luciferase signal was compared after 24 hours post transfection. E, Western blotting showed that addition of IMD-0354 reduced the expression of p-IKKα/□ in BEL7402 D972 cells (*left*). Inhibition of p-IKKα/□ activity abolished the promotion of cell migration (*middle*) and invasiveness (*right*) of BEL7402 cells by D972. F~~E~~, Transient knockdown of p65 by siRNA against p65 in BEL7402 D972 cells as revealed by western blotting (*left*). Suppression of p65 expression abrogated the promotion of cell migration (*middle*) and invasiveness (*right*) of BEL7402 cells by D972. Results are expressed as mean □ SD. Three independent experiments were performed. *P*-value less than 0.05 is regarded as statistically significant.

Figure 6.

Suppression of TAK1 expression abrogated the promoting activity of D972 in MHCC97L cells. A, Expression of TAK1 in MHCC97L D972 stable clone was knocked down by shRNA. Suppression of TAK1 in stable clones, shTAK1#32 and shTAK#34 was confirmed by western blotting and qPCR. Expression of p-p65 was reduced when TAK1 was knocked down. B, Migration (*left*) and invasion (*right*) assay of TAK1 knockdown clones (shTAK1#32 and shTAK#34) established in MHCC97L D972 cells. Values of mean ± SD of triplicates were plotted. Three independent experiments were performed. C, The tumor size was recorded for 5 weeks in subcutaneous injection assay (n = 5 per group) (*left*). D972 shCTL non-target control group showed enhanced tumor formation and formed the biggest tumors (*middle*). TAK1

knockdown clones formed tumors with comparable size as the vector control. The overall weight of the excised tumors (*right*). D, Immunohistochemical staining of TAK1 and p-p65 expressions in excised tumors. E, Orthotopic liver implantation of tumor seed derived from TAK1 knockdown cells (n = 5 per group). Livers were excised at the end of experiment (*left*). Size of liver tumors was measured 5 weeks post liver implantation (*middle*). H&E staining of liver tumors (*right*) (Magnification: 10×). F, Excised lung tissues of D972 shCTL non-target control group showed highest luciferase signal. TAK1 knockdown groups and vector control group showed no signal in lungs (*left* and *middle*). Lung metastasis evaluated according to the luciferase signal (middle). Lungs were examined for metastatic foci by histological analysis. Representative images of H&E stained lung tissues (*right*) (Magnification: 10×). *P*-value less than 0.05 is regarded as statistically significant.

Formatted: Font: Italic

Figure 7. Proposed signaling pathway of nMet. In HCC cells, nMet upregulates TAK1 expression. Enhanced expression of TAK1 phosphorylates IKKβ leading to IκBα phosphorylation and its subsequent proteasomal degradation. Released NF-κB then translocates into the nucleus and activates pro-metastatic genes responsible for HCC cell migration, invasion, tumorigenesis and metastasis.

Figure 1

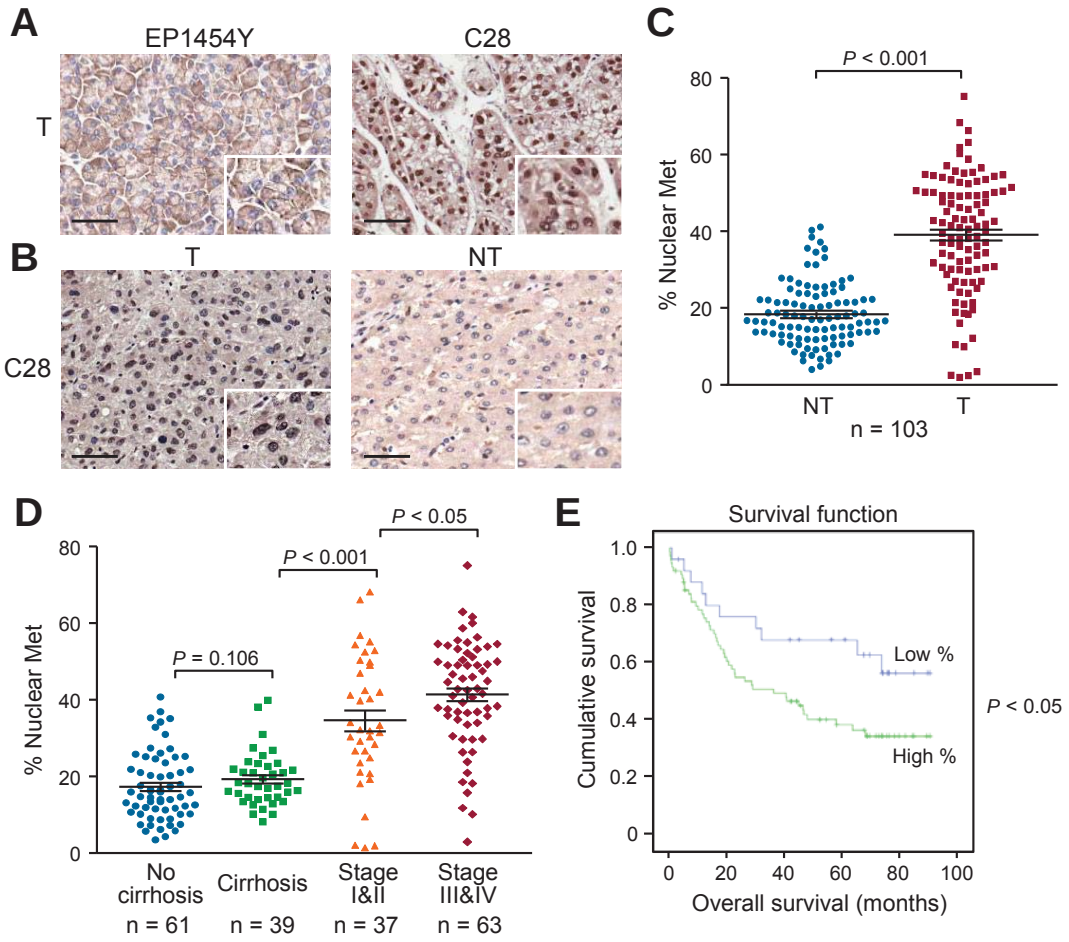
A
EP1454Y
C28
T
B
T
NT
C28
C
P < 0.001
% Nuclear Met
80
60
40
20
0
NT
T
n = 103
D
P < 0.05
P < 0.001
P = 0.106
% Nuclear Met
80
60
40
20
0
No cirrhosis
n = 61
Cirrhosis
n = 39
Stage I&II
n = 37
Stage III&IV
n = 63
E
Survival function
Cumulative survival
1.0
0.8
0.6
0.4
0.2
0
Low %
High %
P < 0.05
0
20
40
60
80
100
Overall survival (months)

Figure 2

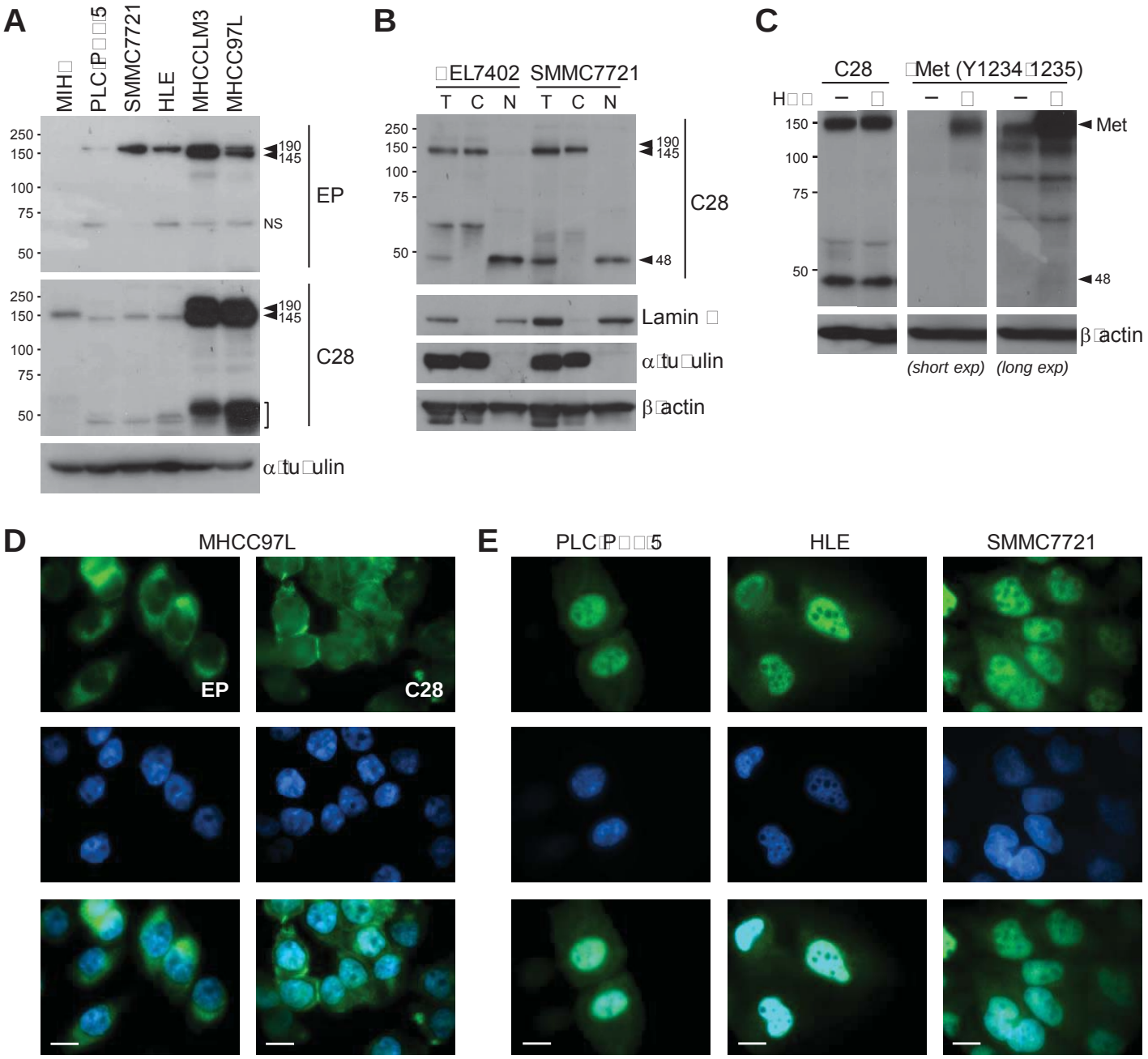
A
MIH
PLC
SMMC7721
HLE
MHCCLM3
MHCC97L
250
150
100
75
50
190
145
EP
NS
C28
α-tubulin
B
EL7402
SMMC7721
T C N T C N
48
C28
Lamin
α-tubulin
β-actin
C
C28
Met (Y1234/1235)
Met
48
β-actin
(short exp)
(long exp)
D
MHCC97L
EP
C28
E
PLC
HLE
SMMC7721

Figure 3

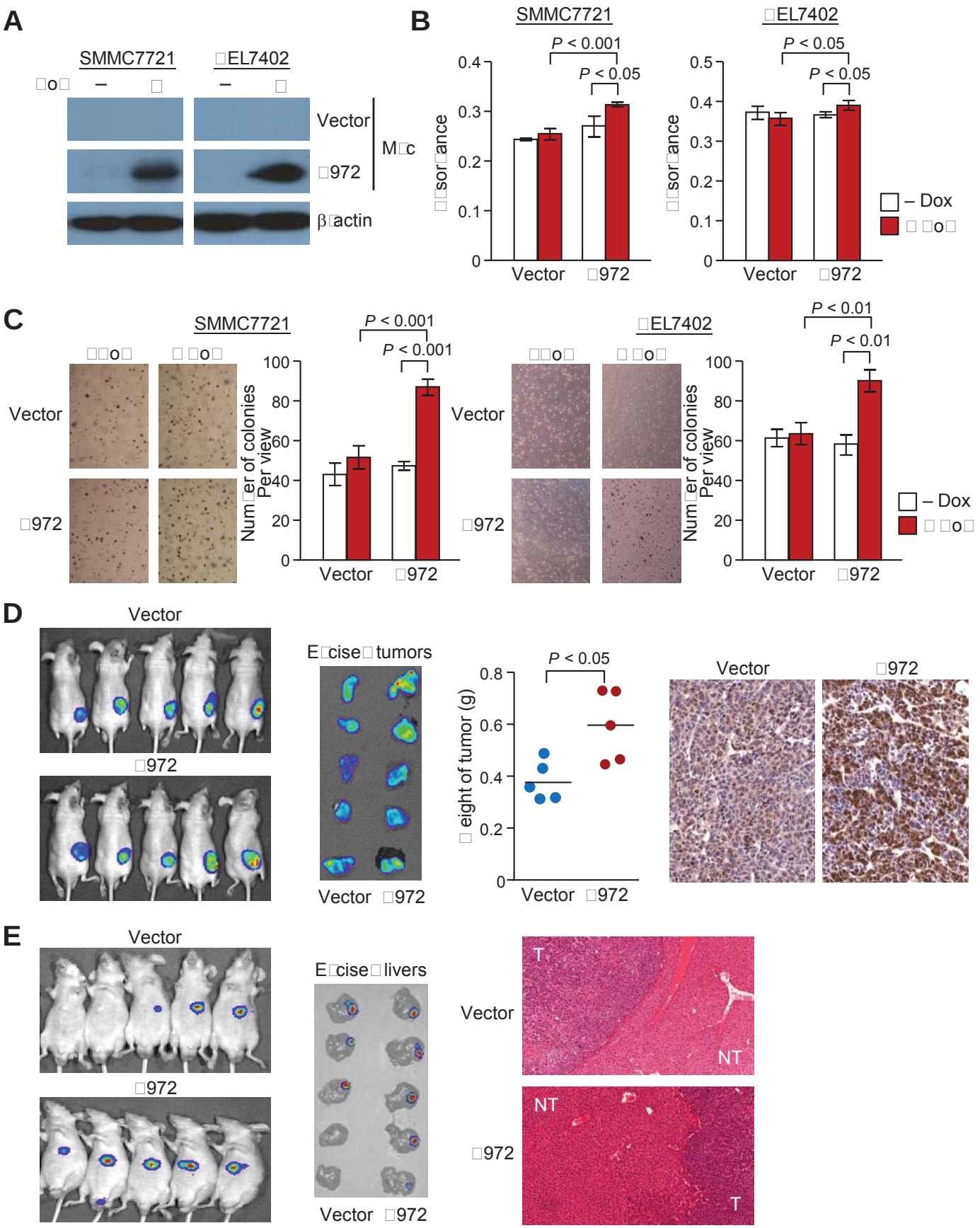
A
SMMC7721
EL7402
Vector
M c
972
actin
B
SMMC7721
EL7402
P < 0.001
P < 0.05
P < 0.05
P < 0.05
Vector
972
– Dox
o
C
SMMC7721
EL7402
P < 0.001
P < 0.001
P < 0.01
P < 0.01
Vector
972
– Dox
o
D
Vector
972
E cise tumors
Vector 972
P < 0.05
Vector
972
E
Vector
972
E cise livers
Vector 972
Vector
T
NT
NT
T

Figure 4

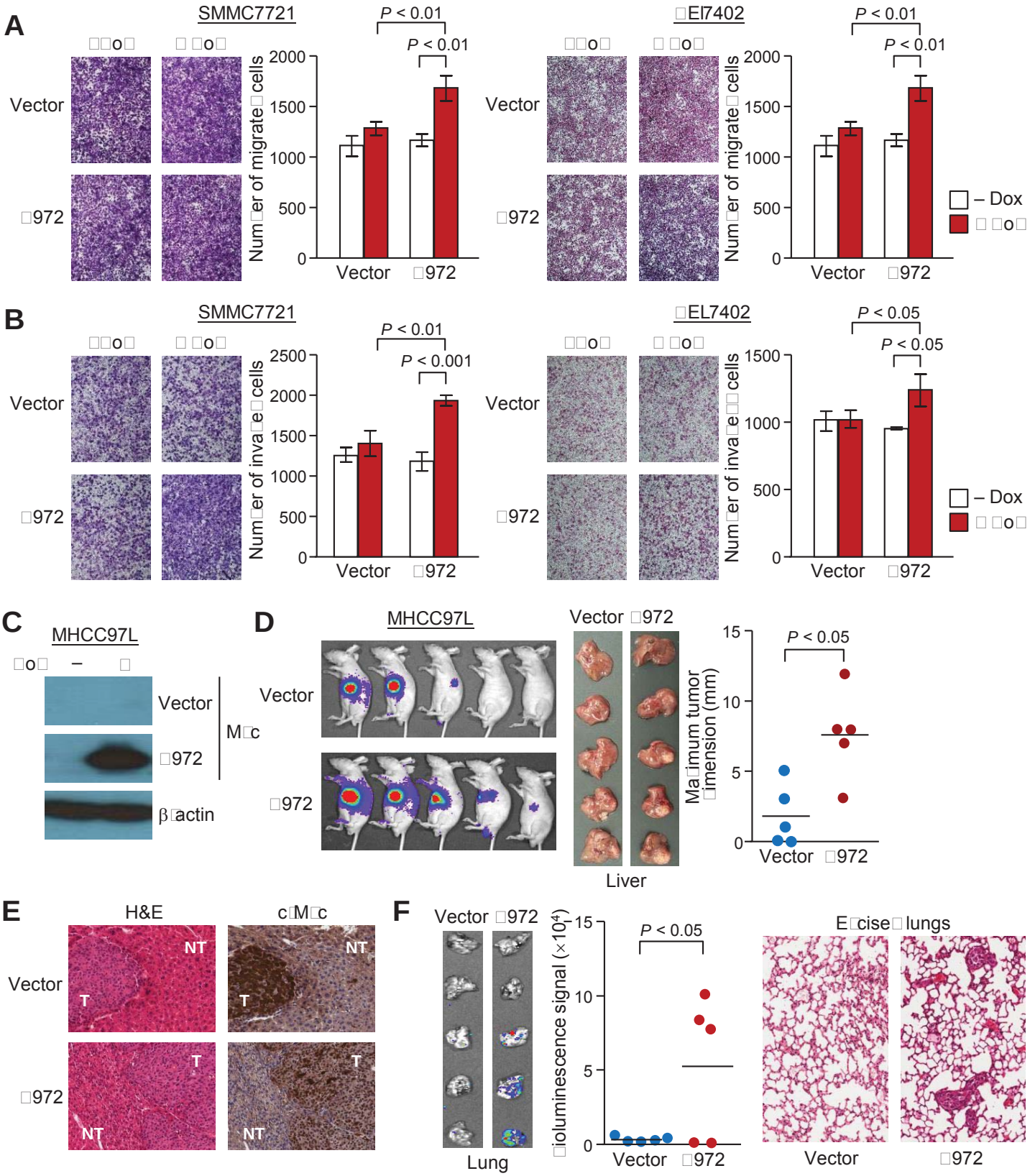
A
SMMC7721
P < 0.01
P < 0.01
Vector
□972
Num□er of migrate□cells
2000
1500
1000
500
0
Vector
□972
– Dox
□ □o□
□El7402
P < 0.01
P < 0.01
B
SMMC7721
P < 0.01
P < 0.001
Num□er of inva□e□cells
2500
2000
1500
1000
500
0
□EL7402
P < 0.05
P < 0.05
C
MHCC97L
□o□ – □
Vector
□972
β□actin
M□c
D
MHCC97L
Vector □972
Vector
□972
Liver
Ma□imum tumor □imension (mm)
15
10
5
0
P < 0.05
E
H&E
c□M□c
Vector
□972
NT
T
F
Vector □972
Lung
□ioluminescence signal (×10⁴)
15
10
5
0
P < 0.05
E□cise□ lungs
Vector
□972

Figure 5

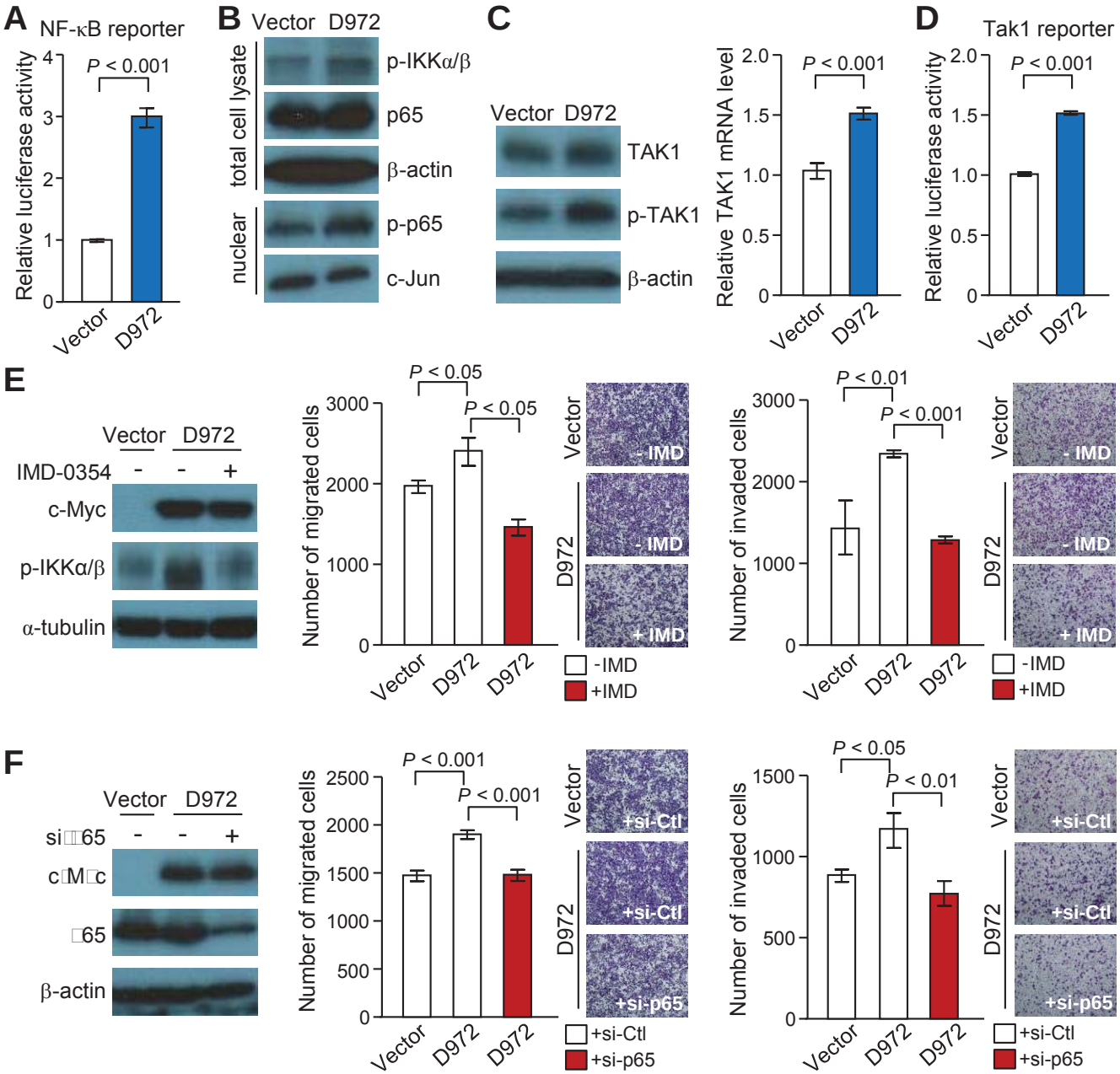
A
NF-κB reporter
Relative luciferase activity
P < 0.001
Vector
D972
B
Vector D972
total cell lysate
nuclear
p-IKKα/β
p65
β-actin
p-p65
c-Jun
C
Vector D972
TAK1
p-TAK1
β-actin
Relative TAK1 mRNA level
P < 0.001
D
Tak1 reporter
Relative luciferase activity
P < 0.001
E
Vector D972
IMD-0354 - - +
c-Myc
p-IKKα/β
α-tubulin
Number of migrated cells
P < 0.05
P < 0.05
Vector
D972
D972
- IMD
+ IMD
-IMD
+IMD
Number of invaded cells
P < 0.01
P < 0.001
F
Vector D972
si□65 - - +
c□M□c
□65
β-actin
Number of migrated cells
P < 0.001
P < 0.001
+si-Ctl
+si-p65
Number of invaded cells
P < 0.05
P < 0.01

Figure 6

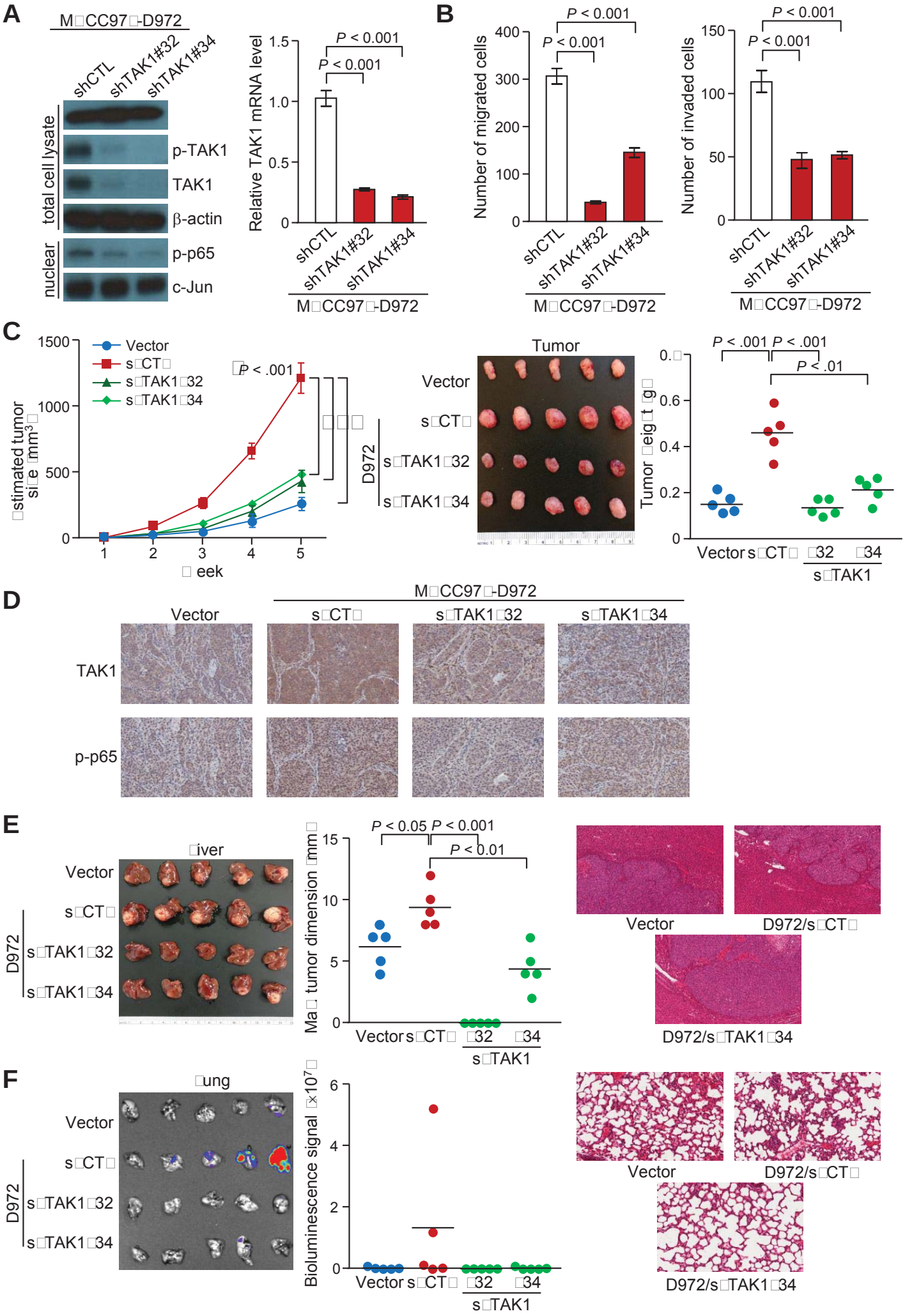
A
M□CC97□-D972
shCTL
shTAK1#32
shTAK1#34
total cell lysate
p-TAK1
TAK1
β-actin
nuclear
p-p65
c-Jun
Relative TAK1 mRNA level
P < 0.001
P < 0.001
shCTL
shTAK1#32
shTAK1#34
M□CC97□-D972
B
Number of migrated cells
P < 0.001
P < 0.001
Number of invaded cells
P < 0.001
P < 0.001
C
Vector
s□CT□
s□TAK1□32
s□TAK1□34
P < .001
D972
□eek
Tumor
Tumor □eig□t □g□
P < .001 P < .001
P < .01
Vector s□CT□ □32 □34
s□TAK1
D
M□CC97□-D972
Vector
s□CT□
s□TAK1□32
s□TAK1□34
TAK1
p-p65
E
□iver
Vector
s□CT□
s□TAK1□32
s□TAK1□34
D972
Ma□ tumor dimension □mm
P < 0.05 P < 0.001
P < 0.01
Vector s□CT□ □32 □34
s□TAK1
Vector
D972/s□CT□
D972/s□TAK1□34
F
□ung
Vector
s□CT□
s□TAK1□32
s□TAK1□34
D972
Bioluminescence signal □×10⁷□
Vector s□CT□ □32 □34
s□TAK1
Vector
D972/s□CT□
D972/s□TAK1□34

Figure 7

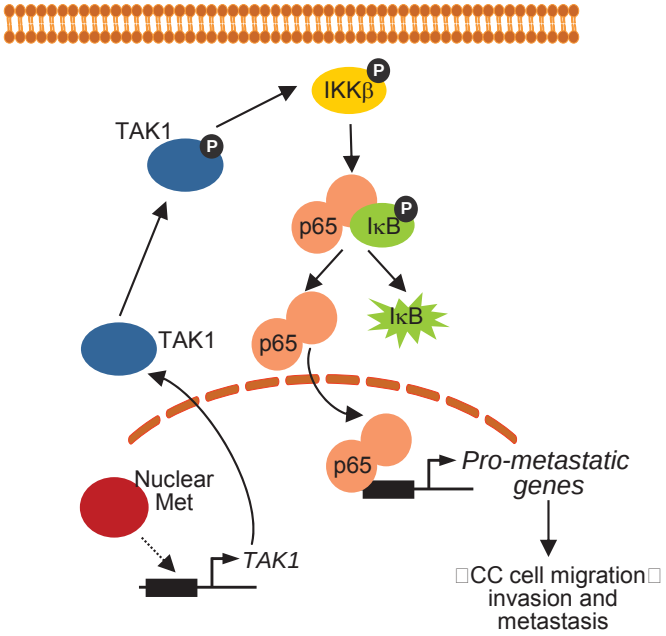
IKKβ
P
TAK1
P
p65
IκB
P
IκB
TAK1
p65
p65
Pro-metastatic genes
Nuclear Met
TAK1
CC cell migration invasion and metastasis

Supplementary File

Click here to download Supplementary File: Nuclear Met supplementary data Cancer Letters Revised unmarked copy.docx

*Conflicts of Interest Statement
Click here to download Conflicts of Interest Statement: Nuclear Met Conflicts of interest Cancer Letters.docx

Conflicts of interest

The authors declare no potential conflicts of interest.

*Revised manuscript untracked

Nuclear Met promotes hepatocellular carcinoma tumorigenesis and metastasis by upregulation of TAK1 and activation of NF-κB pathway

Sze Keong Tey[1], Edith Yuk Ting Tse[1], Xiaowen Mao[1], Frankie Chi Fat Ko[1], Alice Sze Tsai Wong[3], Regina Cheuk-Lam Lo[1,2], Irene Oi-Lin Ng[1,2], Judy Wai Ping Yam[1,2*]

[1]Department of Pathology, Li Ka Shing Faculty of Medicine, The University of Hong Kong, Hong Kong; [2]State Key Laboratory for Liver Research, The University of Hong Kong, Hong Kong; [3]School of Biological Sciences, The University of Hong Kong, Hong Kong

Corresponding author

Judy Wai Ping Yam

Department of Pathology, The University of Hong Kong, University Pathology Building, Queen Mary Hospital, Hong Kong.

Tel: (852) 2255-4864; Fax: (852) 2218-5212; E-mail: judyyam@pathology.hku.hk

Abstract

Presence of Met receptor tyrosine kinase in the nucleus of cells has been reported. However, the functions of Met which expresses in the nucleus (nMet) remain elusive. In this study, we found that nMet was increased in 89% of HCC tumorous tissues when compared with the corresponding non-tumorous liver tissues. nMet expression increased progressively along HCC development and significantly correlated with cirrhosis, poorer cellular differentiation, venous invasion, late stage HCC and poorer overall survival. Western blot analysis revealed that nMet is a 48-kDa protein comprising the carboxyl terminal of Met receptor. Induced expression of nMet promoted HCC cell growth, migration and invasiveness *in vitro* and tumorigenesis and pulmonary metastasis *in vivo*. Luciferase assay showed that nMet activated NF-κB pathway. Indeed, p-IKKα/β and nuclear p-p65 were higher in nMet stable cells than in the control cells. Perturbation of TAK1/NF-κB axis abrogated the aggressiveness of HCC cells, both *in vitro* and *in vivo*. In conclusion, nMet was overexpressed and as a potential prognostic biomarker of HCC. Functionally, nMet accelerated HCC tumorigenesis and metastasis via the activation of TAK1/NF-κB pathway.

Highlights

- nMet is overexpressed in human HCCs and is a potential prognostic factor for HCC patients
- nMet is a truncated cytoplasmic domain of Met surface receptor
- nMet promotes HCC tumorigenesis and metastasis *in vivo*
- Crosstalk between nMet and TAK1/NF-κB pathway leading to the aggressiveness of HCC cells

Keywords

Hepatocellular carcinoma, Metastasis, Nuclear factor kappa B, Nuclear Met, Transforming growth factor beta-activated kinase 1

1. Introduction

Met receptor tyrosine kinase (RTK) is a cell surface single-pass heterodimer comprising a glycosylated extracellular α subunit linked by a disulfide bond to a transmembrane β subunit. Upon binding with its native ligand hepatocyte growth factor (HGF), Met dimerizes and autophosphorylates the cytoplasmic kinase domain, which eventually activates the bidentate substrate binding site and triggers various downstream signaling cascades [1]. Under normal conditions, the HGF-Met axis contributes indispensably with other cytokines and growth factors to coordinate optimal nerve development, liver regeneration, morphogenesis, embryonic development and wound healing [2-5]. However, signaling pathways kindled by aberrant HGF-Met axis orchestrate to switch on the invasive growth program, thereby promoting tumorigenesis, angiogenesis and metastasis in many cancers. Expression level of Met is consistently associated with the progression of different cancers and upregulation of Met is frequently observed in metastatic tumors [6].

Various RTKs, such as ErbB1 and ErbB4, have been reported to translocate into nucleus of cells as either intact or truncated forms [7, 8]. These receptors exert multifaceted functions in different subcellular localizations [9]. Nuclear Met (nMet) was first reported in melanoma tumors and cell lines [10] and was later found in different malignancies, including breast, lung, oral and prostate carcinoma [11-18]. In breast carcinoma, nMet is predictive of poor outcome [12, 19]. These observations suggest the involvement of nMet in oncogenesis. It is intriguing to observe that either full-length or cytoplasmic portions of Met is present in the nucleus of different cellular contexts [20, 21]. Mechanisms underlying the translocation of Met from the cell surface to the nucleus have been suggested. Nuclear translocation of full-length Met has

been induced by HGF [21] while the identification of nuclear localization signal (NLS) in the cytoplasmic fragment of Met supports its entry into the nucleus [22]. Functionally, it has been shown that nMet possesses potential transcriptional activity in MDA-MB231 breast carcinoma cell and initiates calcium signals in SkHep1 cells [20, 21]. A recent paper shows that nMet upregulates SOX9 and activates β-catenin in prostate cancer cells [23]. These findings suggest that in addition to receiving and transducing extracellular signals as a receptor, Met exhibits unexplored capacities in the nucleus. In spite of the importance of Met as the promising therapeutic target in human cancers, the role of nMet in cancers deserves thorough investigation.

In human hepatocellular carcinoma (HCC), Met expression level is higher at both the mRNA and protein level when compared to normal or adjacent non-tumorous liver tissues [24]. Overexpression of Met has been shown to associate with metastasis, invasion and poor prognosis [25, 26]. Functional studies have shown that inhibition of Met activity and expression suppresses HCC cell migration and invasion [27, 28]. Recently, microRNAs have been shown to negatively regulate HCC cell motility by downregulating Met [29, 30]. When Met is co-expressed with c-Myc, hepatocyte proliferation is enhanced and c-Myc-induced tumorigenesis is greatly accelerated [31]. As demonstrated in transgenic mouse model, Met overexpressing hepatocytes readily develop HCC [32]. Another mouse model has shown that expression of the cytoplasmic portion of Met in mouse livers confers resistance to apoptosis [33]. On the contrary, hepatocytes in c-Met conditional knockout mice displayed an enhanced susceptibility to N-nitrosodiethylamine-induced hepatocarcinogenesis when compared to those in control mice [34]. These studies suggest that effects of Met may vary in different stages of carcinogenesis. Although Met has been well documented in HCC, the presence of nMet has not been reported. In the study, we show for the first time the presence and clinical significance of nMet in HCC.

Using different functional assays, nMet was demonstrated to promote HCC cell growth, migration, invasiveness in cell culture model as well as tumorigenesis and distant metastasis in animals. Mechanistically, nMet activates transforming growth factor beta-activated kinase 1 (TAK1) / nuclear factor kappa B (NF-κB) signaling pathway. Perturbation of TAK1/NF-κB pathway abrogates the promoting potential of nMet in HCC. Our study reveal nMet may represent a novel biomarker in HCC and targeting nMet signaling pathway suggests a new therapeutic approach for this aggressive disease.

2. Materials and Methods

2.1. Cell culture, transfection and stable cell lines

Human HCC cell lines, BEL7402 and SMMC7721 were obtained from Shanghai Institute of Cell Biology, Chinese Academy of Sciences, People's Republic of China (PRC). Other HCC cell lines include HLE and PLC/PRF/5 were purchased from American Type Culture Collection (ATCC, Manassas, VA, USA). Metastatic HCC cell lines, MHCCLM3 and MHCC97L were gifts from Fudan University, China. MIHA is an immortalized normal liver cell line and HEK293FT is a normal human embryonal kidney cell line, both were purchased from ATCC. Transfection was performed using either Lipofectamine 2000 (Invitrogen, Gaithersburg, MD, USA) or FuGENE®6 (Roche, Basel, Switzerland) transfection reagent. Lenti-X^{TM} Tet-On$^{®}$ Advanced Inducible Expression System (Clontech, Mountain View, CA, USA) was employed to establish nMet overexpression stable cell lines. A series of N-terminally truncated form of Met, named D972, P1027 and L1157 were designed by PCR (forward primer: D972: 5'-CGGGATCCATGGATGCAAGAGTACACACTCC-3', P1027: 5'-CGGGATCCATGCCTCTGACAGACATGTCCCC-3', L1157: 5'-CGGGATCCATGCTACCATACATGAAACATGG-3'; reverse primer: 5'-CGAATTCTAAATCAGGCTACTGGGCCCAATC-3') using cDNA of the HCC cell line SMMC7221 as the template. A myc tag sequence was added into the expression vector pLVX-Tight-Puro (Clontech) before insertion of D972, P1027 and L1157. The pLVX-Tight-Puro-Myc-D972/P1027/L1157 was transfected into HEK293FT cell for lentivirus packaging. Virus was collected to infect HCC cell lines to establish the stable nMet expressing cell lines. Doxycycline (Clontech) was used to induce the expression of nMet. For TAK1 knockdown experiment,

shTAK1 expression clones were purchased from GeneCopoeia (Rockville, MD, USA).

2.2. Clinical samples and clinicopathological analysis

Paired samples of primary HCC and the corresponding non-tumorous liver tissues from 103 Chinese patients were obtained at the time of surgical resection at Queen Mary Hospital, Hong Kong. Use of human samples was approved by the Institutional Review Board of the University of Hong Kong/Hospital Authority Hong Kong West Cluster (HKU/HA HKW IRB). The association of nMet expression and clinicopathological parameters of the patients was analyzed by Chi-squared test (categorical data) and Mann-Whitney U test (nonparametric continuous data) wherever appropriate. The association of nMet expression with the patients' overall survival rate and disease-free survival rate was examined by Kaplan Meier method. All statistical analyses were performed by IBM SPSS Statistics 23 (SPSS Inc., Chicago, IL) as described. A *P*-value less than 0.05 ($P < 0.05$) is considered to be statistically significant.

2.3. Immunohistochemistry (IHC)

IHC was performed on formalin-fixed, paraffin-embedded liver tissues sections followed by Aperio ScanScope CS System processing. High-quality digital images were created for analysis. The overall intensity of nuclear staining was graded. To determine the percentage of nuclei with positive Met staining, nuclear quantification was performed by the Aperio SlideAnalysis™Toolbox.

2.4. Cell proliferation and soft agar assay

Proliferation rate of adherent cells was determined by BrdU (bromodeoxyuridine) incorporation.

Cells were seeded in a 96-well plate and subjected to BrdU incorporation assay (Roche) according to manufacturer's instructions. Photometric detection was performed in Infinite® F200 microplate reader (Tecan, Maennedorf, Switzerland). Anchorage independent growth of cells was assessed by soft agar assay. The number and size of colonies were evaluated under light microscope. Detailed procedures are described elsewhere.

2.5. Cell migration and invasion assay

Transwell® Permeable Supports (inserts of 6.5 mm in diameter) (Corning, NY, USA) were used for cell migration assay. For cell invasion assay, Transwell® Permeable Supports inserts were coated with BD Matrigel™ Basement Membrane Matrix (BD Bioscience, Beillerica, MA, USA). Cell suspension in serum-free medium was added to the upper chamber at various densities depending on the cell line. Detailed procedures are described elsewhere.

2.6. Subcutaneous injection and orthotopic liver implantation

To perform subcutaneous injection, HCC cells were inoculated into the right flank of male 5-week old BALB/c nude mice. At the end of experiment, tumors were excised and weighed. Tumor seed obtained from subcutaneous injection was used for orthotopic implantation in male BALB/C nude mice. Mice were anesthetized and laparotomy was performed to expose the liver, and the tumor cube was inserted into the liver capsule using a needle. The mice with implanted tumors, which were derived from a luciferase-labeled cell line, were subjected to weekly bioluminescent imaging. Mice were anesthetized and injected with D-luciferin (Xenogen, Hopkinton, MA, USA) before imaging. Images were captured and the bioluminescent signal was quantified using IVIS 100 Imaging System (Xenogen). At the end of experiment, the mice were

sacrificed and their lungs and livers were excised for histological analysis. Animals (Control of Experiments) Ordinance (Hong Kong) and animal experimentation guidance from The University of Hong Kong were strictly followed for all animal work performed.

2.7. Statistical analysis

One-way ANOVA, performed by GraphPad Prism 5 (San Diego, CA, USA), was used for statistical analyses in various functional assays in this study. Clinicopathological analysis was analyzed with Fisher's exact test using IBM SPSS 23 for Windows. A *P*-value less than 0.05 was considered as statistically significant.

Additional experimental procedures are provided in the Supplementary Material and Methods.

3. Results

3.1. nMet was frequently overexpressed and associated with aggressive clinical features and poor prognosis in HCC

Anti-Met antibodies C28, raised against the C-terminal cytoplasmic domain of Met, and EP1454Y, raised against the N-terminal domain of Met, were used to detect Met expression in the nucleus and cytoplasm in HCC tissue samples. EP1454Y antibody detected cytoplasmic expression while C28 antibody revealed both cytoplasmic and intense nuclear stain (Fig. 1A). In 89.3% (92/103) of the paired HCC samples, nMet staining was stronger in tumorous tissues when compared to the corresponding non-tumorous liver tissues (Fig. 1B). The percentage of nuclei with positive Met staining was significantly higher in tumorous tissues (range: 1.48 - 74.89%) than non-tumorous tissues (range: 3.61 - 40.8%) (Fig. 1C; $P < 0.001$; Mann-Whitney U test). nMet expression increased progressively along HCC development (Fig. 1D), with significant increase from the progression of cirrhotic liver (median: 18.19%) to early stage HCC (median: 32.15%) ($P < 0.001$; Mann-Whitney U test), as well as from early to advanced stage HCC (median: 42.71%) ($P < 0.05$; Mann-Whitney U test). A cutoff point was made to segregate the tumorous samples into low (35 cases; range: 1.48 - 33.31%) and high (68 cases; range: 33.32 - 74.89%) percentage of nMet groups. The higher level of nMet was significantly associated with cirrhosis ($P = 0.031$; Chi-squared test), poorer cellular differentiation ($P = 0.019$; Chi-squared test), presence of venous invasion ($P = 0.037$; Chi-squared test), as well as advanced HCC with pTMN stages III-IV ($P = 0.002$; Chi-squared test) (Table 1). Additionally, an association was observed between higher nMet level and poorer overall survival ($P < 0.05$, log-rank test) (Fig. 1E) but not correlated with disease-free survival (data not shown).

3.2. nMet comprised the carboxyl terminus of Met

Expression and subcellular localization of Met was examined in a non-tumorigenic liver cell line MIHA, non-metastatic HCC cell lines PLC/PRF/5, SMMC7221 and HLE, as well as the metastatic HCC cell lines MHCCLM3 and MHCC97L. A band size of around 50-kDa was revealed by C28 antibody but not EP1454 antibody in all HCC cell lines except MIHA, suggesting the protein size of nMet (Fig. 2A). Cellular fractionation revealed that a 48-kDa Met was detected in the total cell lysate as well as the nuclear fraction of BEL7402 and SMMC7221 cells (Fig. 2B), evidently indicating the presence of nMet in HCC cell lines. HGF, the native ligand of Met, did not affect nMet expression. Moreover, phospho-Met antibody detected strong signal of full-length Met but not nMet, suggesting nMet is not phosphorylated under HGF treatment (Fig. 2C). Using immunofluorescence microscopy, membranous and cytoplasmic Met was detected by EP1454Y while, membranous, cytoplasmic as well as nuclear staining was revealed by C28 (Fig. 2D). nMet was also detected in other HCC cells including PLC, HLE and SMMC7221 (Fig. 2E). To examine whether HGF affects the subcellular localization of nMet, we expressed GFP-tagged constructs expressing cytoplasmic fragment of Met (D972, P1027 and L1157). The immunofluorescent staining showed that the nuclear translocation of Met was HGF independent (Supplementary Fig. 1A). RTKs have been shown to shuttle between membrane and nucleus. However, treatment of cells with Leptomycin B (LMB), an inhibitor of CRM1 nuclear exporter, showed that nMet remained static in the nucleus (Supplementary Fig. 1B).

3.3. nMet exerted its functional effect in the nucleus to promote cell proliferation, anchorage independent growth and in vivo tumorigenicity

Based on the size of Met fragment observed in the nuclear lysates of HCC cells (Fig. 2), fragments of Met cytoplasmic fragments were constructed to be expressed in HCC cells for functional characterization (Supplementary Fig. 2A and 2B). Stable inducible clones of nMet were established in SMMC7721 and BEL7402 cells. The expressions of D972, P1027 and L1157 Met cytoplasmic fragments were induced by doxycycline in a time and dosage dependent manner (Supplementary Fig. 2C and 2D). Immunofluorescent staining and cellular fractionation revealed that D972 and P1027 were expressed in the nucleus while L1157 was only detected in the cytoplasm (Supplementary Fig. 3).

BrdU incorporation assay and soft agar assays were performed to study the effect of Met cytoplasmic fragments in HCC cells. Compared with the vector control cells, only D972 significantly promoted cell proliferation (SMMC7721, $P < 0.01$; BEL7402, $P < 0.001$) and anchorage independent growth (SMMC7721, $P < 0.01$; BEL7402, $P < 0.001$) (Supplementary Fig. 4C and 4D). These functional analyses demonstrated that Met cytoplasmic fragments only exerted functional effect when they were expressed in the nucleus. In order to confirm the promoting effect was due to the induced expression of D972, BrdU incorporation assay and soft agar assays were performed on D972 cells established in SMMC7721 and BEL7402 cells treated with or without doxycycline (Fig. 3A). The results revealed that only D972 cells treated with doxycycline showed enhancement in cell proliferation and anchorage independent growth (Fig. 3B and 3C).

In xenograft experiment, BEL7402 D972 cells efficiently promoted tumor formation and resulted in bigger tumors than the vector control ($P < 0.05$) (Fig. 3D). Similar findings were observed in SMMC7721 D972 cells (Supplementary Fig. 5A and 5B). In another experiment, development of tumor derived from SMMC7721 D972 cells was compared in mice fed with or

without doxycycline-containing drinking water. The result showed that larger tumors were formed in mice treated with doxycycline (Supplementary Fig. 5C). This data provided evidence that the promoting effect in tumor formation was due to the doxycycline-induced expression of D972. Solid tumors derived from BEL7402 D972 and control cells in the subcutaneous injection were subjected to orthotopic liver implantation to reveal the growth of tumors in liver. Five weeks after implantation, luciferase imaging revealed a more prominent signal in mice implanted with tumors of D972 when compared to the vector control mice (Fig. 3E). Bigger tumors were found in the liver of D972 group. Tumors of D972 group displayed an invasive growth front by invading adjacent liver tissues. However, such aggressive features were not seen in the tumors of the control group.

3.4. nMet enhanced HCC cell migration, invasiveness and metastasis

Expression of nMet significantly correlated with tumor invasion; a clinical feature of cancer metastasis. This result prompted us to further investigate the functional effect of nMet in HCC cell motility. Consistent with the promoting effect of nMet in cell growth, only D972, but not P1027 and L1157, significantly promoted cell migration (SMMC7721, BEL7402, $P < 0.05$) and cell invasiveness (SMMC7721, $P < 0.001$; BEL7402, $P < 0.01$) (Supplementary Fig. 4E and 4F). Enhancement in cell migration and invasiveness was only evident in D972 cells treated with doxycycline (Figure 4A and 4B). Subsequently, we examined the role of nMet in HCC metastasis by establishing cells with doxycycline-inducible expression of D972, P1027 and L1157 Met cytoplasmic fragments in a metastatic HCC cell line, MHCC97L (Fig. 4C; Supplementary Fig. 6). Similarly, only D972 exerted effect in promoting cell migration and invasion (Supplementary Fig. 7). To examine the effect of D972 in metastasis, tumor seed

derived from MHCC97L D972 and control cells were implanted into liver of mice. Five weeks post implantation, bioluminescence imaging revealed stronger luciferase signal in animals implanted with D972 tumor seed than the control group (Fig. 4D). Consistently, larger liver tumor size was detected in D972 group. The growth fronts of D972 tumors were irregular and invasive, whereas the tumor growth fronts of the control group were found to be bulging and less invasive. The expression of D972 in the tumors was confirmed by immunohistochemistry (Fig. 4E). Moreover, distant lung metastasis and metastatic tumor foci were only observed in lung tissues of D972 group but not in the control group (Fig. 4F).

3.5. nMet activated TAK1/NF-κB pathway

In order to interrogate the molecular mechanism mediated by nMet, various luciferase-conjugated reporters were examined for their activation by Met fragments (Supplementary Fig. 8A). Among all the reporters, D972 could robustly activate NF-κB reporter ($P < 0.001$) (Fig. 5A, Supplementary Fig. 8B). Levels of p-IKKα/β and nuclear p-p65 were higher in BEL7402 D972 stable clone than in the control vector clone (Fig. 5B). We next explored the possibility about the activation of TAK1 by D972. In the stable clone of D972, both TAK1 mRNA and protein levels were upregulated (Fig. 5C). Luciferase reporter carrying TAK1 promoter displayed a higher luciferase activity in D972 cells than in vector control cells (Fig. 5D). To examine whether nMet mediates its functional effects indeed through the activation of TAK1/NF-κB pathway, functional assays of D972 stable clones were performed when NF-κB pathway was perturbed. Treatment of BEL7402 D972 stable clones with IMD-0354, an inhibitor of IKKβ, lowered the expression of p-IKKα/β and the migratory ($P < 0.05$) and invasive ($P < 0.001$) potentials of cells

(Fig. 5E). In addition, knockdown of p65 expression in D972 stable clone reduced cell migration ($P < 0.001$) and invasiveness ($P < 0.05$) (Fig. 5F).

To investigate whether the functional effect of nMet is driven by TAK1, TAK1 stable knockdown clones (shTAK1#32 and shTAK#34) were established in MHCC97L D972 cells. Suppression of TAK1 in MHCC97L D972 cells concomitantly reduced the expression of p-p65 (Fig. 6A). TAK1 knockdown stable clones showed reduced cell migration (shTAK1#32, shTAK1#34, $P < 0.001$) and invasion (shTAK1#32, shTAK1#34, $P < 0.001$) (Fig. 6B). In xenograft experiment, TAK1 knockdown stable clones exhibited slower tumor growth (shTAK1#32, shTAK1#34, $P < 0.001$) and formed smaller tumors (shTAK1#32, shTAK1#34, $P < 0.001$) as compared to non-target control clones (Fig. 6C; Supplementary Fig. 9). IHC staining revealed reduced expressions of TAK1 and p-p65 expressions in excised tumors derived from TAK1 knockdown stable cells (Fig. 6D). Furthermore, potential of TAK1 knockdown stable cells in distant metastasis was studied using orthotopic liver implantation. Five weeks post implantation, smaller liver tumors were found in mice implanted with seed derived from TAK1 knockdown cells (shTAK1#32, $P < 0.001$; shTAK1#34, $P < 0.01$) (Fig. 6E). Histological examination of the livers revealed that tumors of TAK1 knockdown stable clones displayed a less invasive growth front than the tumors in the control group. Moreover, lungs of animals in knockdown group showed no distant metastases. Metastatic tumor foci were only observed in lung tissues of non-target control group (Fig. 6F).

4. Discussion

Aberrant expression and activation of HGF/Met signaling pathway are frequently found in human cancers which make Met an attractive therapeutic target for human cancers. Currently, therapeutic monoclonal antibodies against HGF and Met, as well as small molecule inhibitors antagonizing the kinase activity of Met, are in different phases of clinical trials [35]. The existence and potential functions of Met in the nucleus intelligibly challenge the current therapeutic strategies against Met surface receptor. This situation provides a compelling rationale for obtaining a better understanding about the spatial distribution and roles of Met in different subcellular compartments.

Met localization is not restricted to the cell membrane and cytoplasm. In fact, Met can also be detected in the nucleus. nMet was first observed in melanoma tumors and cell lines independent of HGF [10]. However, Met levels in the nuclei of uveal melanomas and metastatic breast cancer cells are found to be enhanced by HGF stimulation [15, 36]. nMet is also detected in various cancer cell lines [18, 20] and cancerous tissues, particularly at the invasive front [11], suggesting its potential role in human cancers. Interestingly, the distribution pattern of Met is not stagnant. Nuclear translocation of Met may occur in rapidly dividing and not fully differentiated cells [14]. Using antibodies against the carboxyl and amino termini of Met, different outcomes have been observed. Met expression detected by antibodies against the carboxyl terminus of Met is significantly correlated with a poor prognosis in lymph node-negative breast carcinomas. Intriguingly, such correlation is not observed when antibodies targeting the amino terminus of Met are used [12]. Consistent with the reported study, we observed strong nuclear staining in HCC tissues using C28 antibody that directs against the C-terminal of Met (immunogen

sequence: P1366-S1390) whereas EP1454Y antibody, which directs against the extracellular domain of Met, failed to detect such nuclear pattern of Met. Our findings on nMet expression suggest that nMet plays an indispensable role in HCC progression and could be a potential prognostic marker for HCC.

Regardless of the presence of HGF, a 60-kDa fragment of Met that localizes in the nucleus of epidermoid carcinoma cell line is recognized by antibodies against the carboxyl terminus of Met [14]. Due to the absence of a shorter transcript of Met in Northern blot analysis, this study postulates that nMet possibly results from the proteolytic cleavage of full-length Met receptor. In fact, nuclear and cytoplasmic Met of 75 kDa and 85 kDa have been detected in prostate cancer and musculoskeletal tumors, respectively. These observations implicate that the protein size of truncated Met may vary in different cell types. We observed nMet as a 50-kDa protein in various HCC cell lines of different metastatic potentials using C28 antibody. To exclude the possibility that the 50-kDa band is a cross-reacting protein, C12 antibody, which also targets the cytoplasmic domain of Met (immunogen sequence: V1379-S1390), is used to detect proteins immunoprecipitated by C28 antibody. C12 antibody successfully revealed positive signal with the same molecular weight in the nuclear and total cell lysates of HCC cells. Using the same C12 antibody, Met is detected in the nuclear lysate of oral squamous cell carcinoma [18].

Several RTKs are processed by sequential proteolysis which includes shedding of ectodomain by ADAM family of metalloproteinases, followed by cleavage within the transmembrane domain by γ-secretase/presenilin-1/2 [37]. Indeed, ectodomain shedding of Met is specifically inhibited by the tissue inhibitor of metalloproteinase, TIMP-3 [38]. Treatment with γ-secretase inhibitor reduces the accumulation of nMet in prostate cancer cells [23]. In plasma

and urine samples from mice implanted with human tumor xenografts, Met ectodomain fragments are detected. More importantly, the level of soluble Met directly correlates with the tumor volume [39]. In patients with uveal melanoma, higher serum level of soluble Met is found in patients with metastatic disease than those with no sign of metastasis [40]. These findings point to the significance of proteolytic cleavage of Met in cancers. Upon HGF binding, Met has been shown to be internalized and degraded via the formation of endophilin-CIN85-Cbl complex [41]. Proteolytic processing acts as a negative regulatory mechanism to prevent oversignaling of Met; yet it is complicated by the generation of biologically active cytoplasmic fragments of Met. An intracellular 40-kDa fragment, resulted from caspase cleavage of Met, induces apoptosis under stress [42]. Downregulation of Met by presenilin-dependent regulated intramembrane proteolysis also leads to the generation of small labile fragments of Met [43]. Whether and how these cleaved fragments translocate into the nucleus remain to be answered. The nuclear translocation of the cytoplasmic Met fragment has been shown to be regulated by the WW domain-containing oxidoreductase (Wwox) tumor suppressor [20]. Nevertheless, HGF induces nuclear translocation of the full-length Met receptor in a manner that is dependent on the adaptor proteins Gab1 and importin β1 [21]. NLS mediates the translocation of protein molecules larger than 30-40-kDa from the cytoplasm to the nucleus. A recent study mapped a NLS in the juxtamembrane region of Met (H1068-H1079) [22]. This pH-dependent NLS coupled with importin β1 answered the query on how the cytoplasmic fragment of Met can dislocate into the nucleus. We observed that D972 and P1027 but not L1157 localize in the nucleus of HCC cells, suggesting that the region between P1027 and L1157 is responsible for the nuclear translocation of Met. This defined region, which coincides with the location of NLS identified in the previous

study, further supports the NLS-dependent mechanism for directing Met into the nucleus in HCC cells.

Despite the presence of nMet has been reported, its functions remain obscure. Predominant expression of phospho-Met (pMet) in the nucleus of cancerous tissues and cell lines is suggestive that nMet is active [13, 16]. pMet colocalizes with PAX5 transcription factor upon HGF treatment, implying the potential transcriptional activity of nMet [16]. In this perspective, transactivating activity of nMet is further supported by the ability of Met-Gal4 DNA-binding domain fusion protein to transactivate Gal4-luciferase reporter [20]. In our study, doxycycline-induced expression of nMet elevates the transcription of TAK1. However, whether nMet activates TAK1 promoter in a direct or an indirect fashion needs to be further investigated. In our study, P1027 fragment although localizes in the nucleus did not induce similar biological effects as D972 fragment. We suspect that the truncated region of P1072 might affect the biochemical property of nMet. Besides the transactivating activity, nMet has been shown to interact with SMC-1, a chromosome-associated protein, further supports the undefined functional role of Met in the nucleus [44].

Our study discovered a novel mechanism by which nMet mediates the activation of TAK1/NF-κB pathway to drive HCC tumorigenesis and metastasis. nMet overexpression promotes the transcription of TAK1 resulting in the enhanced level of TAK1. Elevated level of TAK1 phosphorylates IKKβ, leading to IκBα phosphorylation and its subsequent proteasomal degradation. Released NF-κB then translocates to the nucleus where it induces transcription of pro-metastatic genes to promote HCC cell migration, invasion and metastasis (Fig. 7). In accordance with the oncogenic role of nMet that we observed in functional studies, nMet overexpression is significantly correlated with HCC patients with advanced tumor stage and

venous invasion, an indication of metastasis (Table 1). TAK1 is an intracellular serine/threonine kinase that regulates both NF-κB and mitogen-activated protein kinase (MAPK) signaling pathways involved in diverse biological processes [45]. TAK1 play a dual role in tumor initiation, progression and metastasis. Disruption of TAK1 in hepatocytes causes hepatic injury, inflammation, fibrosis, and carcinogenesis [46]. Suppression of TAK1 also promotes prostate tumorigenesis [47]. Nevertheless, inhibition of TAK1 prevents lung metastasis of breast cancer [48]. Through the activation of NF-κB signaling, TAK1 enhances the oncogenic capacity of ovarian cancer cells [49]. In one study, HGF has been shown to activate Src leading to the stimulation of NF-κB through TAK1, suggesting that Met as a receptor of HGF is involved in Src-mediated activation of TAK1/NF-κB pathway [50]. Here, we delineate a novel mechanistic pathway showing the connection of nMet and TAK1/NF-κB pathway leading to the progression of HCC.

In this study, we have provided the first evidence about the presence of nMet in HCC which has profound prognostic value. Our findings have also derived new mechanistic insights into hepatocarcinogenesis. More importantly, the expanding knowledge on the signaling networks and actions of Met in the nucleus will provide important insights into the development of therapeutic strategies against aberrant Met in human cancers.

Acknowledgements

We thank the Faculty of Medicine Core Facility for providing Xenogen imaging service for our animal experimentation.

Funding

This work was supported by the Hong Kong Research Grants Council [HKU783613M]; The University of Hong Kong Seed Funding Programme for Basic Research [20111115902] and [201011159041].

Conflicts of interest

The authors declare no potential conflicts of interest.

References

[1] C. Ponzetto, A. Bardelli, Z. Zhen, F. Maina, P. dalla Zonca, S. Giordano, et al. A multifunctional docking site mediates signaling and transformation by the hepatocyte growth factor/scatter factor receptor family. Cell 77 (1994) 261-271.

[2] Y. Uehara, O. Minowa, C. Mori, K. Shiota, J. Kuno, T. Noda, et al. Placental defect and embryonic lethality in mice lacking hepatocyte growth factor/scatter factor. Nature 373 (1995) 702-705.

[3] F. Maina, M.C. Hilton, C. Ponzetto, A.M. Davies, R. Klein. Met receptor signaling is required for sensory nerve development and HGF promotes axonal growth and survival of sensory neurons. Genes Dev 11 (1997) 3341-3350.

[4] J. Chmielowiec, M. Borowiak, M. Morkel, T. Stradal, B. Munz, S. Werner, et al. c-Met is essential for wound healing in the skin. J Cell Biol 177 (2007) 151-162.

[5] M. Borowiak, A.N. Garratt, T. Wustefeld, M. Strehle, C. Trautwein, C. Birchmeier. Met provides essential signals for liver regeneration. Proc Natl Acad Sci U S A 101 (2004) 10608-10613.

[6] C. Birchmeier, W. Birchmeier, E. Gherardi, G.F. Vande Woude. Met, metastasis, motility and more. Nat Rev Mol Cell Biol 4 (2003) 915-925.

[7] C.Y. Ni, M.P. Murphy, T.E. Golde, G. Carpenter. gamma -Secretase cleavage and nuclear localization of ErbB-4 receptor tyrosine kinase. Science 294 (2001) 2179-2181.

[8] S.Y. Lin, K. Makino, W. Xia, A. Matin, Y. Wen, K.Y. Kwong, et al. Nuclear localization of EGF receptor and its potential new role as a transcription factor. Nat Cell Biol 3 (2001) 802-808.

[9] G. Carpenter. Nuclear localization and possible functions of receptor tyrosine kinases. Curr Opin Cell Biol 15 (2003) 143-148.

[10] K. Saitoh, H. Takahashi, N. Sawada, P.G. Parsons. Detection of the c-met proto-oncogene product in normal skin and tumours of melanocytic origin. J Pathol 174 (1994) 191-199.

[11] G. Edakuni, E. Sasatomi, T. Satoh, O. Tokunaga, K. Miyazaki. Expression of the hepatocyte growth factor/c-Met pathway is increased at the cancer front in breast carcinoma. Pathol Int 51 (2001) 172-178.

[12] J.Y. Kang, M. Dolled-Filhart, I.T. Ocal, B. Singh, C.Y. Lin, R.B. Dickson, et al. Tissue microarray analysis of hepatocyte growth factor/Met pathway components reveals a role for Met, matriptase, and hepatocyte growth factor activator inhibitor 1 in the progression of node-negative breast cancer. Cancer Res 63 (2003) 1101-1105.

[13] P.C. Ma, R. Jagadeeswaran, S. Jagadeesh, M.S. Tretiakova, V. Nallasura, E.A. Fox, et al. Functional expression and mutations of c-Met and its therapeutic inhibition with SU11274 and small interfering RNA in non-small cell lung cancer. Cancer Res 65 (2005) 1479-1488.

[14] S. Pozner-Moulis, D.J. Pappas, D.L. Rimm. Met, the hepatocyte growth factor receptor, localizes to the nucleus in cells at low density. Cancer Res 66 (2006) 7976-7982.

[15] M. Ye, D. Hu, L. Tu, X. Zhou, F. Lu, B. Wen, et al. Involvement of PI3K/Akt signaling pathway in hepatocyte growth factor-induced migration of uveal melanoma cells. Invest Ophthalmol Vis Sci 49 (2008) 497-504.

[16] R. Kanteti, V. Nallasura, S. Loganathan, M. Tretiakova, T. Kroll, S. Krishnaswamy, et al. PAX5 is expressed in small-cell lung cancer and positively regulates c-Met transcription. Lab Invest 89 (2009) 301-314.

[17] Y.S. Chen, J.T. Wang, Y.F. Chang, B.Y. Liu, Y.P. Wang, A. Sun, et al. Expression of hepatocyte growth factor and c-met protein is significantly associated with the progression of oral squamous cell carcinoma in Taiwan. J Oral Pathol Med 33 (2004) 209-217.

[18] I.J. Brusevold, T.M. Soland, C. Khuu, T. Christoffersen, M. Bryne. Nuclear and cytoplasmic expression of Met in oral squamous cell carcinoma and in an organotypic oral cancer model. Eur J Oral Sci 118 (2010) 342-349.

[19] S. Pozner-Moulis, M. Cregger, R.L. Camp, D.L. Rimm. Antibody validation by quantitative analysis of protein expression using expression of Met in breast cancer as a model. Lab Invest 87 (2007) 251-260.

[20] E. Matteucci, P. Bendinelli, M.A. Desiderio. Nuclear localization of active HGF receptor Met in aggressive MDA-MB231 breast carcinoma cells. Carcinogenesis 30 (2009) 937-945.

[21] D.A. Gomes, M.A. Rodrigues, M.F. Leite, M.V. Gomez, P. Varnai, T. Balla, et al. c-Met must translocate to the nucleus to initiate calcium signals. J Biol Chem 283 (2008) 4344-4351.

[22] S.C. Chaudhary, M.G. Cho, T.T. Nguyen, K.S. Park, M.H. Kwon, J.H. Lee. A putative pH-dependent nuclear localization signal in the juxtamembrane region of c-Met. Exp Mol Med 46 (2014) e119.

[23] Y. Xie, W. Lu, S. Liu, Q. Yang, B.S. Carver, E. Li, et al. Crosstalk between nuclear MET and SOX9/beta-catenin correlates with castration-resistant prostate cancer. Mol Endocrinol 28 (2014) 1629-1639.

[24] J.J. Gao, Y. Inagaki, X. Xue, X.J. Qu, W. Tang. c-Met: A potential therapeutic target for hepatocellular carcinoma. Drug Discov Ther 5 (2011) 2-11.

[25] P. Kaposi-Novak, J.S. Lee, L. Gomez-Quiroz, C. Coulouarn, V.M. Factor, S.S. Thorgeirsson. Met-regulated expression signature defines a subset of human hepatocellular carcinomas with poor prognosis and aggressive phenotype. J Clin Invest 116 (2006) 1582-1595.

[26] A.W. Ke, G.M. Shi, J. Zhou, F.Z. Wu, Z.B. Ding, M.Y. Hu, et al. Role of overexpression of CD151 and/or c-Met in predicting prognosis of hepatocellular carcinoma. Hepatology 49 (2009) 491-503.

[27] H. You, W. Ding, H. Dang, Y. Jiang, C.B. Rountree. c-Met represents a potential therapeutic target for personalized treatment in hepatocellular carcinoma. Hepatology 54 (2011) 879-889.

[28] A. Salvi, B. Arici, N. Portolani, S.M. Giulini, G. De Petro, S. Barlati. In vitro c-met inhibition by antisense RNA and plasmid-based RNAi down-modulates migration and invasion of hepatocellular carcinoma cells. Int J Oncol 31 (2007) 451-460.

[29] N. Li, H. Fu, Y. Tie, Z. Hu, W. Kong, Y. Wu, et al. miR-34a inhibits migration and invasion by down-regulation of c-Met expression in human hepatocellular carcinoma cells. Cancer Lett 275 (2009) 44-53.

[30] A. Salvi, C. Sabelli, S. Moncini, M. Venturin, B. Arici, P. Riva, et al. MicroRNA-23b mediates urokinase and c-met downmodulation and a decreased migration of human hepatocellular carcinoma cells. FEBS J 276 (2009) 2966-2982.

[31] L. Amicone, O. Terradillos, L. Calvo, B. Costabile, C. Cicchini, C. Della Rocca, et al. Synergy between truncated c-Met (cyto-Met) and c-Myc in liver oncogenesis: importance of TGF-beta signalling in the control of liver homeostasis and transformation. Oncogene 21 (2002) 1335-1345.

[32] R. Wang, L.D. Ferrell, S. Faouzi, J.J. Maher, J.M. Bishop. Activation of the Met receptor by cell attachment induces and sustains hepatocellular carcinomas in transgenic mice. J Cell Biol 153 (2001) 1023-1034.

[33] L. Amicone, F.M. Spagnoli, G. Spath, S. Giordano, C. Tommasini, S. Bernardini, et al. Transgenic expression in the liver of truncated Met blocks apoptosis and permits immortalization of hepatocytes. EMBO J 16 (1997) 495-503.

[34] T. Takami, P. Kaposi-Novak, K. Uchida, L.E. Gomez-Quiroz, E.A. Conner, V.M. Factor, et al. Loss of hepatocyte growth factor/c-Met signaling pathway accelerates early stages of N-nitrosodiethylamine induced hepatocarcinogenesis. Cancer Res 67 (2007) 9844-9851.

[35] A. Furlan, Z. Kherrouche, R. Montagne, M.C. Copin, D. Tulasne. Thirty years of research on met receptor to move a biomarker from bench to bedside. Cancer Res 74 (2014) 6737-6744.

[36] S. Previdi, P. Maroni, E. Matteucci, M. Broggini, P. Bendinelli, M.A. Desiderio. Interaction between human-breast cancer metastasis and bone microenvironment through activated hepatocyte growth factor/Met and beta-catenin/Wnt pathways. Eur J Cancer 46 (2010) 1679-1691.

[37] G. Carpenter, H.J. Liao. Trafficking of receptor tyrosine kinases to the nucleus. Exp Cell Res 315 (2009) 1556-1566.

[38] D. Nath, N.J. Williamson, R. Jarvis, G. Murphy. Shedding of c-Met is regulated by crosstalk between a G-protein coupled receptor and the EGF receptor and is mediated by a TIMP-3 sensitive metalloproteinase. J Cell Sci 114 (2001) 1213-1220.

[39] G. Athauda, A. Giubellino, J.A. Coleman, C. Horak, P.S. Steeg, M.J. Lee, et al. c-Met ectodomain shedding rate correlates with malignant potential. Clin Cancer Res 12 (2006) 4154-4162.

[40] G. Barisione, M. Fabbi, A. Gino, P. Queirolo, L. Orgiano, L. Spano, et al. Potential Role of Soluble c-Met as a New Candidate Biomarker of Metastatic Uveal Melanoma. JAMA Ophthalmol 133 (2015) 1013-1021.

[41] A. Petrelli, G.F. Gilestro, S. Lanzardo, P.M. Comoglio, N. Migone, S. Giordano. The endophilin-CIN85-Cbl complex mediates ligand-dependent downregulation of c-Met. Nature 416 (2002) 187-190.

[42] B. Foveau, C. Leroy, F. Ancot, J. Deheuninck, Z. Ji, V. Fafeur, et al. Amplification of apoptosis through sequential caspase cleavage of the MET tyrosine kinase receptor. Cell Death Differ 14 (2007) 752-764.

[43] B. Foveau, F. Ancot, C. Leroy, A. Petrelli, K. Reiss, V. Vingtdeux, et al. Down-regulation of the met receptor tyrosine kinase by presenilin-dependent regulated intramembrane proteolysis. Mol Biol Cell 20 (2009) 2495-2507.

[44] C.P. Schaaf, J. Benzing, T. Schmitt, D.H. Erz, M. Tewes, C.R. Bartram, et al. Novel interaction partners of the TPR/MET tyrosine kinase. FASEB J 19 (2005) 267-269.

[45] Y.S. Roh, J. Song, E. Seki. TAK1 regulates hepatic cell survival and carcinogenesis. J Gastroenterol 49 (2014) 185-194.

[46] S. Inokuchi, T. Aoyama, K. Miura, C.H. Osterreicher, Y. Kodama, K. Miyai, et al. Disruption of TAK1 in hepatocytes causes hepatic injury, inflammation, fibrosis, and carcinogenesis. Proc Natl Acad Sci U S A 107 (2010) 844-849.

[47] M. Wu, L. Shi, A. Cimic, L. Romero, G. Sui, C.J. Lees, et al. Suppression of Tak1 promotes prostate tumorigenesis. Cancer Res 72 (2012) 2833-2843.

[48] D.M. Ray, P.H. Myers, J.T. Painter, M.J. Hoenerhoff, K. Olden, J.D. Roberts. Inhibition of transforming growth factor-beta-activated kinase-1 blocks cancer cell adhesion, invasion, and metastasis. Br J Cancer 107 (2012) 129-136.

[49] P.C. Cai, L. Shi, V.W. Liu, H.W. Tang, I.J. Liu, T.H. Leung, et al. Elevated TAK1 augments tumor growth and metastatic capacities of ovarian cancer cells through activation of NF-kappaB signaling. Oncotarget 5 (2014) 7549-7562.

[50] S. Fan, Q. Meng, J.J. Laterra, E.M. Rosen. Role of Src signal transduction pathways in scatter factor-mediated cellular protection. J Biol Chem 284 (2009) 7561-7577.

Table 1. Clinicopathological correlation of nuclear Met expression in human HCC

	Low % (No. of cases)	High % (No. of cases)	*P* value
Sex			
Male	27	54	
Female	8	12	0.606
Age 13-74			
≤ 52 years	17	37	
>52 years	18	30	0.539
Non-tumorous liver status			
Normal	3	2	
Chronic hepatitis/cirrhosis	32	65	0.336
Cirrhosis status			
No cirrhosis	27	36	
Cirrhosis	8	31	0.031*
Tumor size			
≤ 5 cm	11	25	
> 5 cm	24	43	0.666
No. of tumour nodules			
1	31	52	
≥ 2	4	16	0.191
Tumor encapsulation			
Absent	24	45	
Present	9	20	0.817
Cellular differentiation[#]			
I-II	25	31	
III-IV	9	35	0.019*
pTMN stage			
I-II	20	17	
III-IV	14	49	0.002*
Hepatitis B surface antigen			
Absent	5	10	
Present	29	56	1.000
Venous Invasion			
Absent	21	25	
Present	14	42	0.037*
Tumor microsatellite formation			
Absent	19	28	
Present	16	39	0.296
Direct liver invasion[##]			
Absent	16	27	
Present	10	24	0.628

According to Edmondson grading

Invasion of tumor into the adjacent liver parenchyma

* $P < 0.05$

Figure legends

Figure 1.

nMet was overexpressed in HCCs. A, Representative HCC tissues showing differential staining pattern revealed by IHC using C28 and EP1454Y antibodies. Insets showing Met staining in membrane, cytoplasm and nucleus are included (Scale bar: 50 μm). B, An example of HCC patient sample revealed stronger nuclear staining in tumorous (T) tissues than in the corresponding non-tumorous (NT) liver tissues detected by C28 antibody (Scale bar: 50 μm). Insets comparing the staining in the nucleus of T and NT tissues. C, nMet expression in 103 HCC clinical samples was detected by C28 antibody and was scored by the Aperio system. The overall nMet expression was significantly higher in tumorous (T) tissues than in the corresponding non-tumorous (NT) liver tissues. D, Progressive increase in nMet expression during HCC development from non-tumorous livers without cirrhosis (n = 61) and with cirrhosis (n = 39) to early HCC with pTMN stages I&II (n = 37) and advanced HCC with pTMN stages III&IV (n = 63). E, Cases with higher nMet expression had a poorer overall survival. *P*-value less than 0.05 is regarded as statistically significant.

Figure 2.

Expression and subcellular localization of Met in HCC cell lines. A, EP1454Y (EP) and C28 antibodies revealed different banding patterns of Met expression in HCC cell lines. Small band sizes of around 50-kDa were only detected by C28 in all HCC cell lines except MIHA, an immortalized liver cell line. B, Cellular fractionation revealed the presence of Met (48-kDa) in the nuclear fraction of BEL7402 and SMMC7721 cells. C, The 48-kDa band of Met was not

detected by phospho-Met (Y1234/1235) antibody under HGF stimulation. D, Immunofluorescence microscopy revealed that EP1454Y detected both cytoplasmic and membranous Met expression but not nuclear expression of Met, while C28 detected nuclear localization of Met in MHCC97L cells. E, C28 also detected nMet in PLC, HLE and SMMC7721 cells. Scale bar represents 10 μm.

Figure 3.

Doxycycline induced expression of D972 promoted in vitro HCC cell growth, anchorage independent growth and *in vivo* tumorigenesis. A, Expression of D972 in SMMC7721 and BEL7420 cells after 2 μg/ml of doxycycline (Dox) treatment for 24 hours was shown by western blotting. B, Induced expression of D972 upon doxycycline treatment significantly promoted cell proliferation when compared to D972 cells without doxycycline induction, as well as control cells treated with and without doxycycline. C, Induced expression of D972 significantly enhanced anchorage independent growth in SMMC7721 (*left*) and BEL7402 cells (*right*). Values of mean ± SD of triplicates were plotted. Three independent experiments were performed. D, Subcutaneous injection assay revealed that luciferase-labeled BEL7402 cells induced with D972 expression promoted tumor formation (n = 5 per group) (*left*). The overall weight of tumors of D972 group was significantly higher than that of the vector control group (*middle*). Immunohistochemistry staining confirmed the expression of induced nMet expression in D972 group but not in vector control group (*right*) (Magnification: 10×). E, Orthotopic liver implantation of tumor seed derived from BEL7402 D972 and control cells (n = 5 per group). Luciferase signal was higher in animals implanted with D972 tumor seed (*left*). Higher luciferase

signal was observed in the liver of D972 group (*middle*). H&E staining of liver tumors (*right*) (Magnification: 10×). Data with *P*-value less than 0.05 is considered as statistically significant.

Figure 4.

Doxycycline induced expression of D972 promoted HCC cell migration, invasiveness and metastasis. Induced expression of D972 promoted (A) cell migration and (B) cell invasiveness in SMMC7721 (*left*) and BEL7402 cells (*right*). Results are expressed as mean ± SD. Three independent experiments were performed. C, Stably transduced cells of metastatic MHCC97L were treated with 2 μg/ml Dox for 24 hours. Induced expression of Myc-tagged D972 was confirmed by western blot analysis using anti-Myc antibody. D, Orthotopic liver implantation of MHCC97L D972 clone resulted in stronger luciferase signal in animals implanted with tumor seed derived from D972 cells (*left*). D972 tumor seed formed significantly larger tumor in liver than the control tumor seed (n = 5 per group) (*middle* and *right*). E, H&E and immunohistochemistry staining of liver tumors (Magnification: 10×). F, Excised lung tissues showed higher incidence of distant metastases in animals implanted with D972 tumor seed than the control group (*left*). Lung metastasis evaluated according to the luciferase signal (*middle*). Lungs were excised and examined for metastatic foci by histological analysis. Representative images of H&E stained lung tissues (*right*) (Magnification: 10×). *P*-value less than 0.05 is regarded as statistically significant.

Figure 5.

D972 activated TAK1/NF-κB pathway. A, Expression constructs of D972 and NF-κB reporter were co-expressed in HEK293 cells. Luciferase activity was measured 24 hours post transfection.

D972 significantly activated NF-κB reporter. B, Higher nuclear p-p65 and p-IKKα/β expressions were detected in the D972 stable clone when compared to the control stable clone. C, TAK1 expression in BEL7402 D972 stable clone was analyzed by western blotting and qPCR. D, Luciferase reporter carrying TAK1 promoter was expressed in MHCC97L vector and D972 cells and the luciferase signal was compared after 24 hours post transfection. E, Western blotting showed that addition of IMD-0354 reduced the expression of p-IKKα/β in BEL7402 D972 cells (*left*). Inhibition of p-IKKα/β activity abolished the promotion of cell migration (*middle*) and invasiveness (*right*) of BEL7402 cells by D972. F, Transient knockdown of p65 by siRNA against p65 in BEL7402 D972 cells as revealed by western blotting (*left*). Suppression of p65 expression abrogated the promotion of cell migration (*middle*) and invasiveness (*right*) of BEL7402 cells by D972. Results are expressed as mean ± SD. Three independent experiments were performed. *P*-value less than 0.05 is regarded as statistically significant.

Figure 6.

Suppression of TAK1 expression abrogated the promoting activity of D972 in MHCC97L cells. A, Expression of TAK1 in MHCC97L D972 stable clone was knocked down by shRNA. Suppression of TAK1 in stable clones, shTAK1#32 and shTAK#34 was confirmed by western blotting and qPCR. Expression of p-p65 was reduced when TAK1 was knocked down. B, Migration (*left*) and invasion (*right*) assay of TAK1 knockdown clones (shTAK1#32 and shTAK#34) established in MHCC97L D972 cells. Values of mean ± SD of triplicates were plotted. Three independent experiments were performed. C, The tumor size was recorded for 5 weeks in subcutaneous injection assay (n = 5 per group) (*left*). D972 shCTL non-target control group showed enhanced tumor formation and formed the biggest tumors (*middle*). TAK1

knockdown clones formed tumors with comparable size as the vector control. The overall weight of the excised tumors (*right*). D, Immunohistochemical staining of TAK1 and p-p65 expressions in excised tumors. E, Orthotopic liver implantation of tumor seed derived from TAK1 knockdown cells (n = 5 per group). Livers were excised at the end of experiment (*left*). Size of liver tumors was measured 5 weeks post liver implantation (*middle*). H&E staining of liver tumors (*right*) (Magnification: 10×). F, Excised lung tissues of D972 shCTL non-target control group showed highest luciferase signal. TAK1 knockdown groups and vector control group showed no signal in lungs (*left* and *middle*). Lung metastasis evaluated according to the luciferase signal (middle). Lungs were examined for metastatic foci by histological analysis. Representative images of H&E stained lung tissues (*right*) (Magnification: 10×). *P*-value less than 0.05 is regarded as statistically significant.

Figure 7. Proposed signaling pathway of nMet. In HCC cells, nMet upregulates TAK1 expression. Enhanced expression of TAK1 phosphorylates IKKβ leading to IκBα phosphorylation and its subsequent proteasomal degradation. Released NF-κB then translocates into the nucleus and activates pro-metastatic genes responsible for HCC cell migration, invasion, tumorigenesis and metastasis.